

Perceptual spaces and their symmetries: The geometry of color space

Nicolás Vattuone¹²³⁴, Thomas Wachtler¹² and Inés Samengo³⁴

1. Department of Biology II, Ludwig-Maximilians-Universität München, Germany.
2. Bernstein Center for Computational Neuroscience, Munich, Germany.
3. Department of Medical Physics, Centro Atómico Bariloche, Argentina.
4. Instituto Balseiro, Centro Atómico Bariloche, Argentina.

Abstract

Our sensory systems transform external signals into neural activity, thereby producing percepts. We are endowed with an intuitive notion of similarity between percepts, that need not reflect the proximity of the physical properties of the corresponding external stimuli. The quantitative characterization of the geometry of percepts is therefore an endeavour that must be accomplished behaviorally. Here we characterized the geometry of color space using discrimination and matching experiments. We proposed an individually tailored metric defined in terms of the minimal chromatic difference required for each observer to differentiate a stimulus from its surround. Next, we showed that this perceptual metric was particularly adequate to describe two additional experiments, since it revealed the natural symmetry of perceptual computations. In one of the experiments, observers were required to discriminate two stimuli surrounded by a chromaticity that differed from that of the tested stimuli. In the perceptual coordinates, the change in discrimination thresholds induced by the surround followed a simple law that only depended on the perceptual distance between the surround and each of the two compared stimuli. In the other experiment, subjects were asked to match the color of two stimuli surrounded by two different chromaticities. Again, in the perceptual coordinates the induction effect produced by surrounds followed a simple, symmetric law. We conclude that the individually-tailored notion of perceptual distance reveals the symmetry of the laws governing perceptual computations.

1 Introduction

The neural computations involved in conscious perception, reflections about the world, and action planning, are not performed on external stimuli, but rather on our internal representations of those stimuli. To execute such computations, we are endowed with an intuitive notion of similarity between stimuli. For example, we can typically tell whether two faces are alike or not, whether two tools are exchangeable, or whether two colors are more or less similar. This ability suggests that percepts can be modeled as elements of an abstract space equipped with a notion of distance, so that similar objects are close to each other. If percepts and neural representations capture regularities of our sensory environment in a manner appropriate for behavior (von Helmholtz, 1896; Barlow, 2001), one could expect that perceptual similarity has a correspondence in the physical world.

The notion of conceptual spaces has been explored by several studies recently, proposing that, for example, the entorhinal-hippocampal network represents not only spatial information, but more generally, abstract cognitive spaces. A whole variety of cognitive spaces have been investigated, ranging from simple attributes of sensory stimuli (Aronov et al., 2017; Radvanski and Dombek, 2018), to highly complex notions, as bird shape (Constantinescu et al., 2016) or social hierarchy (Kumaran et al., 2016). The hypothesis is that the items represented in these spaces satisfy geometric constraints such as betweenness and equidistance, so that properties and concepts occupy convex regions (Bellmund et al., 2018). The geometric aspects of physical space are thus attributed to other spaces, and are conjectured to be functionally relevant to guide imagination (Horner et al., 2018; Bellmund et al., 2016) and decision making (Kaplan et al., 2017).

Yet, a priori, the existence of an intuitive notion of similarity between a collection of items does not guarantee that the items be describable as points in a space endowed with a topology or a geometry, let alone a Riemannian geometry, in which distances and angles obey exact mathematical relations, and surfaces or volumes can be measured quantitatively. The existence of a proper geometry has to be verified experimentally. In this paper, we go through such verification. Following Resnikoff (1974), we work specifically with the space of colors, although the procedure is also valid for other conceptual spaces.

We first describe the correspondence between items in the external world and items in the internal representation. This step is important, since the mapping need not be one-to-one. In

the case of colors, chromatic contexts cause whole collections of external stimuli to be mapped onto single percepts. Once the correspondence is characterized, and the elements of the perceptual space are identified, the geometric structure of percepts is inferred. We first assume that colors form a manifold, that is, a topological space that can be locally and smoothly mapped to \mathbb{R}^n . This assumption is grounded on the observation that any pair of colors can be connected by a trajectory containing colors whose physical and perceptual attributes vary continuously. By definition, a differential manifold comes with an Atlas, that is, the set of all the possible coordinate charts over the manifold. Any such system of coordinates may be employed to parametrize the chromaticity of visual stimuli, and the choice does not alter the perceived color.

Next, for similarity to reflect a geometric property of percepts, the manifold must be endowed with a distance. Importantly, while a mathematical notion of distance can always be imposed, the question remains whether a distance exists that describes perceptual effects in the simplest possible manner, a goal that has been overlooked so far. Assuming such distance exists, the resulting geometry may or may not be Riemannian, that is, it may or may not result from a metric tensor. If it is, then the set of points that are all at the same (infinitesimal) distance from a given chosen point conform an ellipsoid, from which the metric tensor can be derived. Moreover, in the vicinity of each given point, a special coordinate system known as the “normal coordinates” exists, in which the first derivatives of the metric vanish, making the geometry to appear locally flat. In General Relativity, the existence of normal coordinates is the mathematical formulation of the equivalence principle, stating that in a free falling - or inertial - system, spacetime is locally flat. If, additionally, the Riemannian manifold has zero curvature, in the normal coordinates the metric tensor becomes the identity everywhere, so the perceptual distance becomes Euclidean. In this paper, the normal coordinates are called “perceptual”, since they are derived from perceptual experiments. In these coordinates the symmetries of perception are most naturally revealed, just as Euclidean coordinates of physical space are the ones that most simply reveal the symmetries of Newtonian dynamics.

One of the laws governing color perception establishes that the presence of a chromatic context surrounding a stimulus modifies the perceived color of the stimulus (Jameson and Hurvich, 1964; Ware and Cowan, 1982; Wachtler et al., 2001). For example, a green stimulus appears more yellowish when surrounded by cyan, and more bluish when surrounded by orange. This effect implies that the function that transforms the activities of photoreceptors into a higher-level representation of color depends on the chromaticity of the surround. The perceptual shift is repulsive, since the presence of the surround shifts the perceived stimulus color in color space away from that of the surround (Eichengreen, 1976; Ware and Cowan, 1982; Smith and Poko-

ny, 1996; Wachtler et al., 2001; Ekroll et al., 2004; Hansen et al., 2007). The shift is also non-uniform, since its magnitude, when reported in any of the color coordinates normally used in colorimetry, varies from location to location in color space (Klauke and Wachtler, 2015). Moreover, the inhomogeneity of color space is also evident in the variation of just-noticeable differences obtained in discrimination experiments throughout color space (MacAdam, 1942; Witzel and Gegenfurtner, 2013). The question remains, however, whether inhomogeneities could perhaps vanish with an adequate choice of the coordinate system, as has been claimed with theoretical arguments (da Fonseca and Samengo, 2018). If such were the case, a privileged system of coordinates would exist, revealing a fundamental symmetry of the space of colors. In this paper, the ability of an observer to discriminate neighboring colors is used to define a perceptual system of coordinates individually tailored for each observer. In the perceptual coordinates, the shift in color induced by surrounds is approximately homogeneous and isotropic, supporting the hypothesis that the perceptual coordinates reveal properties of the space in which chromatic stimuli are represented internally, and in which contrast-induced computations are performed.

To derive the perceptual coordinates we first determined discrimination thresholds along the S and $L - M$ cardinal directions. We then measured how such thresholds were modified by chromatic surrounds, and confirmed the homogeneity and isotropy of the effect when expressed in the perceptual coordinates. Finally, we measured the color shifts induced by chromatic surrounds by performing asymmetric matching experiments, in which the colors to be matched were presented against surrounds of different chromaticities. The shifts can be modeled as the consequence of a repulsive field that, in the perceptual coordinates, is isotropic around the surround color. Color perception, therefore, exemplifies the fact that percepts, though belonging to the realm of subjective experience, may exhibit elegant mathematical symmetries when described in the adequate coordinates and with the proper geometry.

2 Methods

2.1 Stimuli

Stimuli were displayed on a 21-inch Sony GDM F520 CRT screen, controlled by an 8-bit ATI Radeon HD 4200 graphics card. The spatial resolution was 1280×1024 pixels and the refresh rate 85 Hz. The display was calibrated using a PhotoResearch (Chatsworth, CA) PR-655

spectroradiometer controlled by the IRIS software (Kellner and Wachtler, 2016). Photoreceptor excitations $(\bar{S}, \bar{M}, \bar{L})$ of a given stimulus were obtained by linearly filtering the stimulus spectrum with the Stockman and Sharpe (2000) cone fundamentals. To define the stimuli, a neutral gray was chosen as reference (luminance = 105 cd/m², CIE[x, y] = [0.328, 0.328]), with coordinates $(\bar{S}_g, \bar{M}_g, \bar{L}_g) = (1.48, 40.9, 75.1)$. The cone contrast coordinates of a stimulus were defined as

$$(S, M, L) = \left(\frac{\bar{S} - \bar{S}_g}{\bar{S}_g}, \frac{\bar{M} - \bar{M}_g}{\bar{M}_g}, \frac{\bar{L} - \bar{L}_g}{\bar{L}_g} \right).$$

These coordinates are invariant under scaling of each of the cone fundamentals. To increase chromatic resolution, stimulus patches were filled with a spatially randomized mixture of pixels with four integer 8-bit *RGB* values. Each pixel was colored with one of the four integer *RGB* values closest to the target fractional *RGB*. The four options were chosen in appropriate proportions. As neighboring colors were indistinguishable at the resolution of single pixels, the patches appeared uniform to subjects.

All measurements were performed along the two cardinal chromatic axes (Fig. 1C): the *S* axis, here denoted as x_1 and defined by the condition $L = M = 0$, and the $L - M$ axis (x_2), defined by the conditions $S = 0$ and $L + M = 0$.

2.2 Subjects

Seven subjects (4 female, 3 male), aged between 22 and 32 participated in the experiments. Subjects gave written consent for participation. Three of the subjects were informed about the purpose of the study and performed measurements along both cardinal color space axes. The remaining four were naïve with respect to the study and performed measurements along a single cardinal color space axis each, either $x_1 = S$ or $x_2 = L - M$. All observers had normal color vision as assessed by the Farnsworth–Munsell 100 Hue test, and had normal or corrected to normal visual acuity.

2.3 Procedure

The experiments were performed in a darkened room. Subjects were seated and viewed the display from a distance of 90 cm. The size of the screen was 40 × 30 cm, subtending a solid angle of 25° × 19°. Subjects were instructed to fix their gaze on a black circle displayed at the

center of the screen. Each experiment began with at least 2 min of adaptation to the lighting conditions, during which the subject received instructions and performed test trials that were not included in the analysis.

2.3.1 Experiments *I* and *II*: Discrimination

Experiments *I* and *II* determined the minimal chromatic difference that stimuli need to bear in order for an observer to identify them as different. The task for the observer was to detect the one out of four stimuli that was chromatically different from the other three. In *Experiment I*, the chromaticity of the three equal stimuli coincided with that of the surround, whereas in *Experiment II*, all stimuli were different from the surround.

A session consisted of 300 trials, lasting for approximately 10 minutes. Throughout a session, the chromaticity \mathbf{b} of the surround remained fixed and constantly displayed. At the beginning of each trial, a black circle appeared as a fixation point at the center of the screen. After 500 ms, four 2° square patches were displayed for 150 ms at a center-to-center distance of 2° from the fixation point along the cardinal directions. Three of the patches were colored with the test color \mathbf{x} . The fourth patch was the target patch and had a slightly different color $\tilde{\mathbf{x}}$. The location of the target patch was varied randomly from trial to trial among the four alternatives. The observer was required to report its position using arrow keys on a keyboard. Subjects had unlimited time to respond. They were allowed to freely set the pace of the experiment by triggering each trial with a key on the keyboard. In each session, the tested color \mathbf{x} remained fixed, and the altered color $\tilde{\mathbf{x}}$ was chosen randomly among 15 alternatives around \mathbf{x} , each sampled 20 times.

In *Experiment I*, the color of the surround coincided with that of the three test patches (Fig. 1A), so the observer had to detect the location of the target patch in a uniform surround. In *Experiment II*, the surround \mathbf{b} had a different chromaticity, so the observer had to compare the four patches, and detect the target patch (Fig. 1B). In both experiments, the color of the surround was varied systematically along the $b_1 = S$ and the $b_2 = L - M$ dimensions, while the luminance $L + M$ was maintained constant (Sect. 2.1). In *Experiment I*, each time the surround \mathbf{b} was modified, the tested color \mathbf{x} was changed accordingly. Eight different chromaticities were tested along each axis (values in Fig. 5). In *Experiment II*, colors of stimuli and surrounds were varied independently. Three surround chromaticities were employed on each cardinal axis, with cone contrast coordinates $S = -0.24, 0, 0.16$, and $L - M = -0.03, 0, 0.03$. Eight different

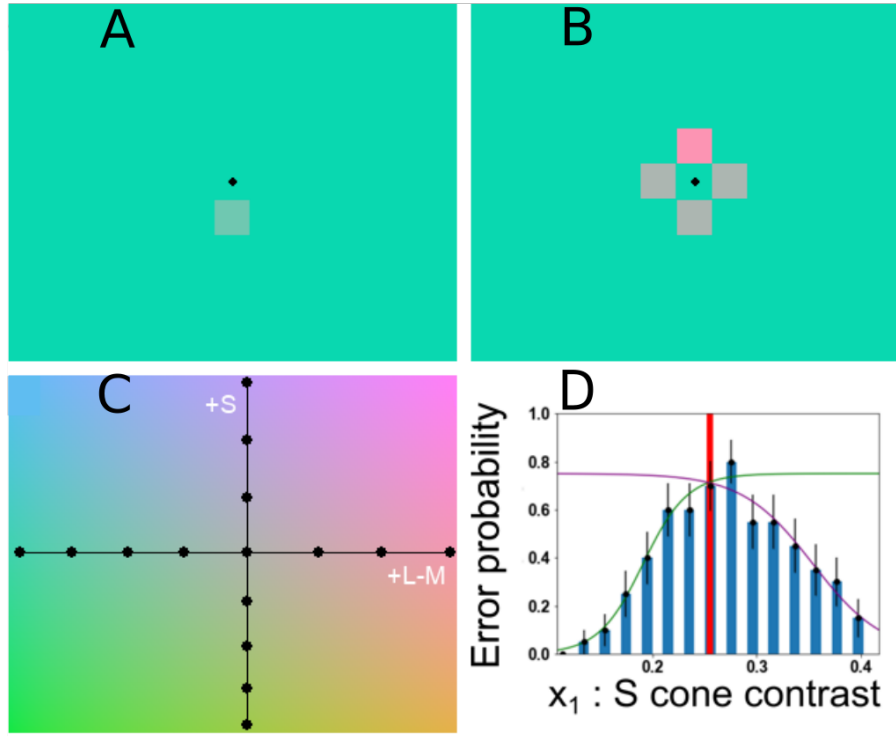


Figure 1: **Experimental paradigms of the discrimination experiments.** (A, B): Stimulus displays for discrimination experiments, performed with surround chromaticity b equal to (A) or different from (B) the tested color x . C: Thresholds were measured for eight tested colors on each axis (black circles). The intersection of the axes corresponds to the reference gray. D: Error probability (black bars) reported by subject S2 in a session of $N = 20$ trials per target stimulus, as a function of the S cone contrast \tilde{x}_1 of the altered stimulus, for a fixed tested stimulus x_1 (red bar). Random responses are expected to produce 75% of incorrect identifications. As the difference $|\tilde{x}_1 - x_1|$ between the dissimilar patch and the other three patches increases, the error probability drops. Error bars denote the standard errors for corresponding binomial distributions. The fitted parameters of Eq. 1 are $a_\ell = 0.043 \pm 0.004$, $b_\ell = 0.191 \pm 0.003$, $a_r = 0.07 \pm 0.01$, $b_r = 0.354 \pm 0.006$.

chromaticities were used for the test stimuli on each axis (Fig. 1 C).

As observers selected one among four options, the chance error rate was 75%. This percentage diminished with increasing discriminability. Figure 1D displays the error probability for subject S2 in a given session for different altered colors \tilde{x} around the tested color x . We defined the discrimination threshold ε as the value of \tilde{x} for which the error probability was equal to the midpoint between pure chance and perfect performance, i.e. when the error probability was 37, 5%. Thresholds may be different for increasing and decreasing cone activation (Chichilnisky and Wandell, 1996), implying that the bar plot of Fig. 1D need not be symmetric around the maximum. In order to take asymmetries into account, left-side (ℓ) and right-side (r)

thresholds were estimated by separately fitting sigmoid functions to the data for each side of the tested color. The fitted functions were

$$P_{\ell,r}(\tilde{x}) = 0.375 [1 \pm \tanh(a_{\ell,r}(\tilde{x} - b_{\ell,r}))], \quad (1)$$

with fitted parameters a_ℓ and b_ℓ or a_r and b_r for the left and right side, respectively. The left (decreasing cone contrast) and right (increasing cone contrast) thresholds of a the reference color x were defined as $\Delta_{\ell,r} = |b_{\ell,r} - x|$, and the mean threshold, as $\varepsilon = (\Delta_\ell + \Delta_r)/2$.

2.3.2 Experiment 3: Asymmetric matching

Colored surrounds alter the perceived color of a test stimulus (Klauke and Wachtler, 2015). To test these influences along the cardinal color axes, we performed *Experiment III*, an asymmetric color matching task. In these experiments, test and match stimuli were displayed in surrounds of different chromaticities. In classical color matching experiments (Commission Internationale de l’Eclairage, 1932; Guild, 1932; Stiles and Burch, 1959; Wyszecki and Stiles, 1982), subjects performed the match to the test stimulus by adjusting the match stimulus without constraints on fixation or presentation time. To control for these factors, and to work in conditions that were similar to those of the discrimination experiments, we used a forced-choice paradigm. In each trial, the observer was presented two candidate patches on one half of the screen surrounded by color b^β , and was instructed to select among them the one perceived as most similar to the target patch displayed on the other half of the screen, surrounded by color b^α (Fig. 2A). The side of the screen occupied by the target patch was randomized in each trial.

For each combination of test stimulus x^α in surround b^α , here denoted as $x^\alpha \parallel b^\alpha$, the aim was to determine the match x^β on the surround b^β . In other words, we searched for the color x^β that fulfilled the perceptual equality $x^\beta \parallel b^\beta \sim x^\alpha \parallel b^\alpha$. Here, the symbol “ \sim ” means that stimulus x^α surrounded by b^α appears to have the same chromaticity as stimulus x^β surrounded by b^β . The search for x^β was performed as a staircase procedure (Sect. 2.3.3).

Three pairs of surrounds were used for each axis. Two of the pairs combined the neutral reference gray corresponding to the color space origin with the maximally and minimally attainable coordinates on the axis, respectively. The cone contrasts of these surrounds with respect to the neutral gray were $S_{\min} = -0.35$, $S_{\max} = 0.25$ for axis S, and $L - M_{\min} = -0.20$, $L - M_{\max} = 0.15$ for axis L-M. The third pair did not include gray, and contained the two other surrounds of *Experiment II* that were unsaturated colors in cardinal directions. Their cone con-

trasts with respect to the neutral gray were $S = -0.24$ and $S = 0.16$ for axis S , $L - M = -0.03$ and $L - M = 0.03$ for axis $L - M$. The first two pairs were useful to assess the shifts produced by fairly saturated colors, and to measure the structure of the induction when the distance between the colored and neutral surround was large. The third pair was selected so as to connect the results of *Experiment III* with those of *Experiment II*, and to assess the behavior of the shift for desaturated surrounds.

Subjects initiated each trial by pressing a key on the keyboard. At the beginning of each presentation both surrounds were shown for 200 ms, together with a black circle as fixation point. Then, a patch of color x^α was presented on b^α and two patches with colors x^p and x^q appeared against the surround b^β , one above the other (top and bottom locations randomized) for 500 ms. All patches subtended a visual angle of 2° . After the stimulus presentation, a masking stimulus was displayed for 500 ms, consisting of randomly sized and located square patches with a balanced distribution of colors along the corresponding axis, to reduce afterimages (Wachtler et al., 2001). Then, the uniform neutral gray background was displayed, and the subject was required to respond whether the top or the bottom patch (x^p or x^q) was most similar to x^α by pressing the corresponding arrow key on the keyboard.

2.3.3 Staircase procedure

Experiment III was structured in sequences, one sequence defined as 6 consecutive trials. In each trial, two patches with colors x^p and x^q appeared on the surround b^β . The subject's task was to select the patch that appeared to be most similar to the target x^α , presented against the surround b^α . The two options x^p and x^q were meant to be an upper and a lower bound for the matched color x^β , and were updated progressively throughout the trials forming a sequence. In the first trial of the sequence, x_1^p and x_1^q took the maximal and minimal values allowed by the display for the corresponding axis. For instance, along the $x_1 = S$ axis, initially x_1^p was a maximally saturated purple and x_1^q , a maximally saturated yellow-green. At trial i , the subject decided whether $x_i^p \parallel b^\beta$ or $x_i^q \parallel b^\beta$ was perceived as more similar to $x^\alpha \parallel b^\alpha$. For trial $i + 1$, the non-selected bound at step i was updated by the midpoint between the two previous options, that is,

$$\begin{aligned} x_{i+1}^p &= x_i^p - (1 - z_i) \frac{x_i^p - x_i^q}{2} \\ x_{i+1}^q &= x_i^q + z_i \frac{x_i^p - x_i^q}{2} \end{aligned}$$

where $z_i = 0$ if the subject chose x_i^p , and $z_i = 1$, otherwise. Both progressions of chromaticities x_i^p and x_i^q were bounded and monotonic, and their distance decreased exponentially, so they both converged to the same value x^β . We estimated this value as $(x_6^p + x_6^q)/2$, and interpreted as the color for which $x^\beta \parallel b^\beta$ matched $x^\alpha \parallel b^\alpha$. We verified that after 6 steps, the two bounds were indistinguishable.

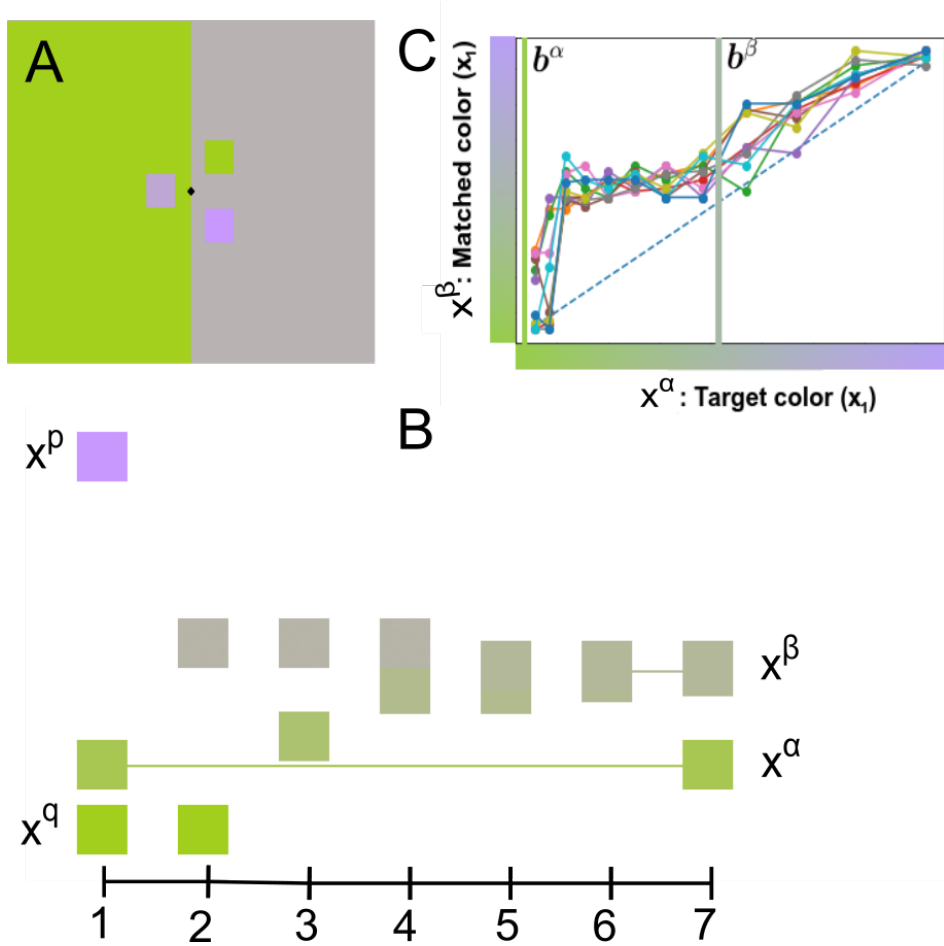


Figure 2: **Experimental paradigm of the matching experiments.** A: Two patches x^p and x^q were presented on the right, surrounded by b^β . The observer had to report which of the patches appeared most similar to the target stimulus x^α on the left, which was surrounded by b^α . B: Sequence of chromaticities x^p and x^q appearing in response to the choices of the subject. Horizontal axis: trial sequence. Vertical axis: coordinate $S = x_1$ of each patch. Horizontal line: target color x^α . The staircase sequence contained 6 trials, after which the final matched stimulus x^β was calculated as the average of x_6^p and x_6^q . C: Chromaticity x^β presented on surround b^β (gray line) that matched the target x^α presented on surround b^α (green line). Different lines represent the converged chromaticity obtained in each of the 10 sequences responded by observer S2.

2.4 The perceptual coordinates

Discrimination thresholds can be understood as the granularity with which the space of colors is perceived. The underlying assumption is that the neural activities involved in representing two colors separated by less than the threshold are not reliably different. Yet, the size of thresholds, and their variation throughout color space, depend on the coordinate system. In this paper, we report the experimental results in the cone contrast coordinates $x_1 = S$ and $x_2 = L - M$ (Derrington et al., 1984), maintaining the total luminance $x_3 = L + M$ fixed, as done in previous studies (Klaue and Wachtler, 2015). Each color is represented as a column vector \mathbf{x} with components x_1 and x_2 . In order to reveal the symmetries of color space, we use the measured thresholds to define a metric tensor J , and the perceptual coordinates (x'_1, x'_2) of each observer. In this section, we show how to transform from the cone contrasts to the perceptual coordinates.

The metric tensor $J(\mathbf{x})$ of the space of colors must be symmetric and non-negative. The line element $d\ell$ measuring the distance between a given color \mathbf{x} and the infinitesimally displaced color $\mathbf{x} + d\mathbf{x}$ is

$$\begin{aligned} d\ell &= \text{Dist}(\mathbf{x}, \mathbf{x} + d\mathbf{x}) \\ &= \sqrt{d\mathbf{x}^t J(\mathbf{x}) d\mathbf{x}} \\ &= \sqrt{J(\mathbf{x})_{11} (dx_1)^2 + 2 J(\mathbf{x})_{12} dx_1 dx_2 + J(\mathbf{x})_{22} (dx_2)^2}, \end{aligned} \tag{2}$$

where the superscript t represents vector transposition. Our aim is to find the tensor $J(\mathbf{x})$ that represents perceptual differences, that is, the one for which the distance $d\ell$ of Eq. 3 between two neighboring colors \mathbf{x} and $\mathbf{x} + d\mathbf{x}$ captures their behavioral discriminability. If an observer is capable of particularly accurate discrimination between \mathbf{x} and a slightly displaced color along a direction $\hat{\mathbf{e}}$, the discrimination threshold must be particularly small in this direction. The smaller the threshold, the more sensitive the observer. It therefore makes sense to define perceptual distances inversely proportional to discrimination thresholds.

To construct $J(\mathbf{x})$, the discrimination threshold between color \mathbf{x} and a displaced color along the direction $\hat{\mathbf{e}}$ needs to be measured for every possible direction $\hat{\mathbf{e}}$. Operationally, this means to move progressively away from \mathbf{x} , in small steps that add up to ε , along the direction $\hat{\mathbf{e}}$, and to test whether the reached color $\mathbf{x} + \varepsilon \hat{\mathbf{e}}$ can be discriminated from \mathbf{x} with a pre-set accuracy. If this is the case, then \mathbf{x} and $\mathbf{x} + \varepsilon \hat{\mathbf{e}}$ are defined to be at a fixed distance from each other. In this paper, we define the units of length by setting this distance as equal to 1: A length of one unit in color space is equal to a pre-set discrimination accuracy (see Sect. 2.3.1, where the

threshold accuracy is defined). If the reached color cannot be discriminated from \mathbf{x} , the size of ε is increased, and the procedure is iterated until the first color that passes the test is reached.

If thresholds are assumed to vary continuously with the direction $\hat{\mathbf{e}}$, the lowest-order analytical expression that captures their directional modulation is given by the equation of an ellipse, obtained by setting the distance $d\ell$ of Eq. 3 equal to 1 and squaring the resulting equality. The vector $(\varepsilon\hat{\mathbf{e}})^t = (\varepsilon_1, \varepsilon_2)$ is therefore a solution of

$$(\varepsilon\hat{\mathbf{e}})^t J(\mathbf{x}) \varepsilon\hat{\mathbf{e}} = \begin{pmatrix} \varepsilon_1 & \varepsilon_2 \end{pmatrix} \begin{pmatrix} J_{11}(\mathbf{x}) & J_{12}(\mathbf{x}) \\ J_{21}(\mathbf{x}) & J_{22}(\mathbf{x}) \end{pmatrix} \begin{pmatrix} \varepsilon_1 \\ \varepsilon_2 \end{pmatrix} = 1, \quad (3)$$

which defines an ellipse because of the positive definiteness of J . The eigenvectors of $J(\mathbf{x})$ are aligned with the principal axes of the ellipse, and the eigenvalues are the inverse square of their lengths. An ellipse centered at point \mathbf{x} is determined by three non-colinear points, or equivalently by the length of its semiaxes and its orientation. Therefore, by measuring the discrimination thresholds along three directions, and using Eq. 3, a system of three equations and three unknowns is obtained, the solution of which are the components of the symmetric tensor J .

The length of a path connecting two remote colors is obtained by integrating local increments $d\ell$ along the trajectory. Conceptually, this means that the total length is the number of thresholds that need to be crossed to travel from one color to the other. Of course, the metric tensor may vary along the path, and different paths connecting the same pair of points may have different lengths. The distance is then defined as the length of the shortest path. For practical reasons, $J(\mathbf{x})$ cannot be estimated for the infinite collection of points \mathbf{x} composing the trajectory. In order to calculate the path integral, hence, $J(\mathbf{x})$ must be estimated for a subset of colors \mathbf{x} that sample the curve under study with sufficient resolution. The intermediate tensors are then interpolated under the assumption that the discrimination ability varies continuously between samples.

Under adaptation to the surround, the results of Krauskopf and Gegenfurtner (1992) indicated that, in the cone contrast coordinates, the diagonal terms of $J(\mathbf{x})$ vanish. In this case, thresholds only need to be measured along the cardinal axes \mathbf{e}^1 and \mathbf{e}^2 . Infinitesimal distances along the axes then read

$$\begin{aligned} d\ell_i &= \text{Dist} [\mathbf{x}, \mathbf{x} + dx_i \mathbf{e}^i] \\ &= \sqrt{J_{ii}(\mathbf{x}) (dx_i)^2} \\ &= \frac{|dx_i|}{\varepsilon(\mathbf{e}^i)}, \end{aligned} \quad (4)$$

where the subscript i indicates either the S ($i = 1$) or the $L - M$ ($i = 2$) coordinate. The distance between two colors \mathbf{x}^a and $\mathbf{x}^b = \mathbf{x}^a + \Delta \mathbf{e}^i$ that differ by a vector aligned with the cardinal axes i is found by integration

$$\begin{aligned} \text{Dist} [\mathbf{x}^a, \mathbf{x}^b] &= \int_{\mathbf{x}^a}^{\mathbf{x}^b} d\ell \\ &= \int_{\mathbf{x}^a}^{\mathbf{x}^b} \sqrt{J_{ii}(\mathbf{x})} |dx_i| \end{aligned} \quad (5)$$

If $J(\mathbf{x})$ is diagonal, and in addition, the term $J_{ii}(\mathbf{x})$ only depends on the component x_i (as verified by Krauskopf and Gegenfurtner (1992)), the space of colors has zero curvature. In this case, a coordinate transformation $\mathbf{x} \rightarrow \mathbf{x}'$ exists, such that the transformed metric is Euclidean. In Euclidean spaces, all geodesics are straight lines, which greatly simplifies the perceptual shift produced by surrounds, as explained below. In the new coordinates, the discrimination ability of the observer is isotropic and homogeneous, that is, all discrimination ellipses become circles, and all circles have the same size. These are the coordinates that most naturally reveal the perceptual abilities of the subject, and are therefore here called the *perceptual* coordinates of the observer. It is easy to prove that the function instantiating the transformation to the perceptual coordinates is

$$\begin{aligned} x'_1(\mathbf{x}) &= d[(x_1^0, x_2^0)^t, (x_1, x_2)^t] \\ &= \int_{x_1^0}^{x_1} \sqrt{J(y_1, x_2^0)} dy_1, \end{aligned} \quad (6)$$

$$\begin{aligned} x'_2(\mathbf{x}) &= d[(x_1^0, x_2^0)^t, (x_1^0, x_2)^t] \\ &= \int_{x_2^0}^{x_2} \sqrt{J(x_1^0, y_2)} dy_2, \end{aligned} \quad (7)$$

where $d(\mathbf{x}^p, \mathbf{x}^q)$ is the distance between colors \mathbf{x}^p and \mathbf{x}^q , and \mathbf{x}^0 is the origin of the new system of coordinates ($\mathbf{x}'(\mathbf{x}^0) = \mathbf{0}$) and may be chosen arbitrarily.

3 Results

3.1 Classes of equivalence in the space of stimuli \times surrounds

In this paper, we assess the effect of context on percepts using color perception as a paradigmatic example. First we describe the mapping between external stimuli and percepts, with special

emphasis on the role of context. For the sake of simplicity, the only aspect of context that matters is chromaticity, all other aspects (as spatial or temporal structure) are kept uniform. The color with which a stimulus is perceived depends on the spectral properties of both the stimulus and the surround. Mathematically, this means that

$$\text{Perceived color} = \text{Function}[\mathbf{x}, \mathbf{b}], \quad (8)$$

where \mathbf{x} and \mathbf{b} represent the stimulus and the surround, respectively. In trichromats, three numbers suffice to characterize the perceivable properties of the power spectrum, giving rise to the well-known 3-dimensional color spaces, such as *LMS*, *RGB*, *XYZ*, or others. Equation 8 implies that, in order to specify a percept, 6 coordinates are required, 3 for the color of the stimulus and 3 for the surround.

Quite remarkably, although chromatic surrounds modify the way stimuli are perceived, the percept they induce is still a color, since observers engage themselves naturally in asymmetric matching experiments, where they match pairs of stimuli surrounded by different colors. This means that for each stimulus \mathbf{x}^α presented against surround \mathbf{b}^α , and for each new surround \mathbf{b}^β , a new stimulus \mathbf{x}^β can be defined by a function

$$\mathbf{x}^\beta = \Phi_{\mathbf{b}^\alpha \rightarrow \mathbf{b}^\beta}(\mathbf{x}^\alpha), \quad (9)$$

such that

$$\mathbf{x}^\alpha \parallel \mathbf{b}^\alpha \sim \mathbf{x}^\beta \parallel \mathbf{b}^\beta.$$

In asymmetric matching experiments, observers compute the function $\Phi_{\mathbf{b}^\alpha \rightarrow \mathbf{b}^\beta}$. As first noted by Resnikoff (1974), the matching operation “ \sim ” defines an equivalence relation, that is, a relation between pairs of “stimulus \parallel surround” that is reflexive ($\mathbf{x} \parallel \mathbf{b} \sim \mathbf{x} \parallel \mathbf{b}$), symmetric (if $\mathbf{x}^\alpha \parallel \mathbf{b}^\alpha \sim \mathbf{x}^\beta \parallel \mathbf{b}^\beta$ then $\mathbf{x}^\beta \parallel \mathbf{b}^\beta \sim \mathbf{x}^\alpha \parallel \mathbf{b}^\alpha$), and transitive (if $\mathbf{x}^\alpha \parallel \mathbf{b}^\alpha \sim \mathbf{x}^\beta \parallel \mathbf{b}^\beta$ and also $\mathbf{x}^\beta \parallel \mathbf{b}^\beta \sim \mathbf{x}^\gamma \parallel \mathbf{b}^\gamma$, then $\mathbf{x}^\alpha \parallel \mathbf{b}^\alpha \sim \mathbf{x}^\gamma \parallel \mathbf{b}^\gamma$). All equivalence relations induce a partition in the set they operate upon. In other words, the set of pairs $\mathbf{x} \parallel \mathbf{b}$ can be segmented into disjoint subsets, or *classes of equivalence*. All pairs belonging to the same class are pairwise connected with the relation \sim , and also, pairs belonging to different classes are not connected with \sim . In line with Resnikoff, here we assume that a given *color* is the percept shared by all the pairs that belong to the same class. A color is therefore not a property of a specific stimulus \mathbf{x} , nor even of a specific pair $\mathbf{x} \parallel \mathbf{b}$. It is a property of a whole class of pairs. In mathematical terms, color is the quotient space of the original space of pairs and the equivalence relation “ \sim ”. Therefore, the 6 coordinates mentioned above constitute a redundant representation of color. Classes of equivalence are 3-dimensional submanifolds embedded in the 6-dimensional space defined by stimuli and surrounds. If selecting a color is equivalent to selecting a class, 3

coordinates suffice. In Fig. 3, the classes of equivalence are illustrated for four different choices for the function defining the displacements induced by surrounds. Since it is not possible to depict 3-dimensional submanifolds embedded inside a 6-dimensional space, the figure shows slices containing the axes (x_1, b_1) and (x_2, b_2) , respectively. In these slices, each class appears as a curve. In Fig. 3A, the surround does not alter the perceived color of the stimulus, and

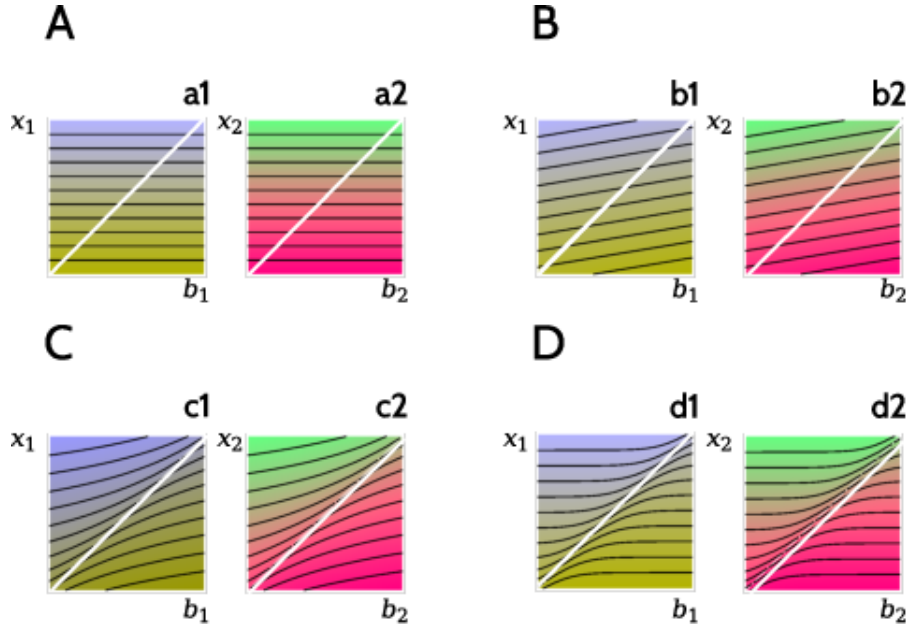


Figure 3: **Classes of equivalence.** Four different examples of the structure of the partition induced by classes of equivalence. Black lines represent classes of equivalence, and are obtained by plotting $\Phi_b(x)$ for fixed x (one value per line) and varying b . The diagonal white line contains the uniform representatives. A: The surround does not alter the color of the stimulus, so the classes of equivalence are planar (straight lines). B: The surround induces a linear classes of equivalence, as suggested by Resnikoff (1974) and Provenzi (2020). C and D: Two other possible partitions of color space, with more complex classes of equivalence.

therefore, the classes of equivalence are planar: Irrespective of the surround, $x \parallel b$ is always perceived the same. In Fig. 3B, classes of equivalence are linear. The surround produces a repulsive effect, which becomes larger as the distance between the surround and the stimulus increases. In panels C and D, the effect of the surround is more complex.

We now assume that, [at least for the unsaturated colors explored in this paper](#), all equivalence classes contain a unique *uniform representative*, that is, a pair of the form $x \parallel x$, in which the stimulus coincides with its surround. In Fig. 3, uniform representatives lie along the white diagonal line, so the assumption means that all classes intersect the diagonal. The hypothesis is supported by the empirical observation that subjects find feasible the task of matching a uniform stimulus $x \parallel x$ of controlled chromaticity with a target stimulus x' presented against a

surround of different chromaticity \mathbf{b}' . In our lab, this feasibility has been verified for the set of target stimuli that can be produced by our computer screen. Although this set does not include maximally saturated colors, it is broad enough to encompass a rich collection of chromaticities. The uniform representative of each class must be unique, since all the members of a class are perceptually indistinguishable, and two uniform representatives of different chromaticity are (by definition of “different”) distinguishable. We define the function $\Phi_{\mathbf{b}}(\mathbf{x})$ as the one that maps each member $\mathbf{x} \parallel \mathbf{b}$ of a given class to its uniform representative $\mathbf{x}^0 \parallel \mathbf{x}^0$, such that

$$\mathbf{x}^0 = \Phi_{\mathbf{b}}(\mathbf{x}), \Leftrightarrow \mathbf{x} \parallel \mathbf{b} \sim \mathbf{x}^0 \parallel \mathbf{x}^0. \quad (10)$$

If, when shown on a fixed surround \mathbf{b} , the stimuli \mathbf{x}^α and \mathbf{x}^β are perceived as different, then they necessarily belong to different classes, and $\Phi_{\mathbf{b}}$ maps them to different uniform representatives. Therefore, for fixed \mathbf{b} , the function $\Phi_{\mathbf{b}}(\mathbf{x})$ must be injective. Since $\mathbf{x} \parallel \mathbf{b}$ and $\mathbf{x}^0 \parallel \mathbf{x}^0$ belong to the same class, the functions $\Phi_{\mathbf{b}}$ and $\Phi_{\mathbf{b}^\alpha \rightarrow \mathbf{b}^\beta}$ must obey the relation

$$\Phi_{\mathbf{b}^\alpha \rightarrow \mathbf{b}^\beta} = \Phi_{\mathbf{b}^\beta}^{-1} \circ \Phi_{\mathbf{b}^\alpha}, \quad (11)$$

where the symbol \circ represents function composition, so that $\Phi_{\mathbf{b}^\beta}^{-1} \circ \Phi_{\mathbf{b}^\alpha}(\mathbf{x}_\alpha) \equiv \Phi_{\mathbf{b}^\beta}^{-1}[\Phi_{\mathbf{b}^\alpha}(\mathbf{x}_\alpha)]$. The injectivity of $\Phi_{\mathbf{b}}$ guarantees that the inverse $\Phi_{\mathbf{b}}^{-1}$ exists.

Uniform representatives remain unchanged by Φ , that is, $\Phi_{\mathbf{x}}(\mathbf{x}) = \mathbf{x}$, for all \mathbf{x} . The uniqueness of uniform representatives implies that all the points along the diagonal correspond to different classes, and that classes must cross the diagonal once and only once.

3.2 A notion of distance in color space

From the above considerations, it follows that any notion of distance between colors must be expressible as a notion of distance between classes of equivalence. In this paper, we start by defining a distance $d(\mathbf{x}^\alpha \parallel \mathbf{x}^\alpha, \mathbf{x}^\beta \parallel \mathbf{x}^\beta)$ between uniform representatives, that is, along the white diagonal in Fig. 3. To simplify the notation, from now on, whenever the distance function is evaluated on a pair of colors $d(\mathbf{x}^\alpha, \mathbf{x}^\beta)$ – as opposed to a pair of pairs $d(\mathbf{x}^\alpha \parallel \mathbf{b}^\alpha, \mathbf{x}^\beta \parallel \mathbf{b}^\beta)$ – we assume that both colors are uniform representatives, that is,

$$d(\mathbf{x}^\alpha, \mathbf{x}^\beta) := d(\mathbf{x}^\alpha \parallel \mathbf{x}^\alpha, \mathbf{x}^\beta \parallel \mathbf{x}^\beta). \quad (12)$$

The distance between non-uniform stimuli is then inherited from the distance between the corresponding representatives,

$$\begin{aligned} d(\mathbf{x}^\alpha \parallel \mathbf{b}^\alpha, \mathbf{x}^\beta \parallel \mathbf{b}^\beta) &= d[\Phi_{\mathbf{b}^\alpha}(\mathbf{x}^\alpha) \parallel \Phi_{\mathbf{b}^\alpha}(\mathbf{x}^\alpha), \Phi_{\mathbf{b}^\beta}(\mathbf{x}^\beta) \parallel \Phi_{\mathbf{b}^\beta}(\mathbf{x}^\beta)] \\ &= d[\Phi_{\mathbf{b}^\alpha}(\mathbf{x}^\alpha), \Phi_{\mathbf{b}^\beta}(\mathbf{x}^\beta)]. \end{aligned} \quad (13)$$

To calculate the distance between two pairs that do not both lie along the diagonal, we must first slide them through their respective classes of equivalence until they both hit the diagonal (in general, on different places), and then use the definition of distance for uniform representatives.

From the formal point of view, distances can only be defined between classes of equivalence, that is, between elements of the quotient space. Since there is a unique uniform representative per class, the distance is also well defined in the set of uniform representatives. However, the extension to pairs discussed above defines a pseudo-distance, since two different pairs can have zero distance. For simplicity, here we do not make explicit distinction between distances and pseudo-distance, hoping that the context will always make clear which concept is used in each case.

Distances between uniform representatives are defined in terms of just noticeable differences. That is, we define two uniform representatives to be at distance 1 when they are first discriminable with a pre-set accuracy. Stimuli that are closer do not reach the desired discriminability threshold. Each observer has their own individually tailored notion of distance, which we revealed with *Experiment I*. The obtained notion of distance can be used to define the perceptual coordinates, in which classes of equivalence at the discriminability threshold cross the diagonal of Fig. 3 at equi-distant points. In *Experiment II*, we repeat the discrimination experiments, but now with a surround of different chromaticity. The compared stimuli, hence, are no longer uniform representatives. We report the thresholds thus obtained in the perceptual coordinates, and, since the percept of each nonuniform $x \parallel b$ is equivalent to that of some uniform $x^0 \parallel x^0$, the comparison between the two experiments allows us to characterize the function $\Phi_b(x)$. In *Experiment II*, surrounds are fairly close to stimuli, so the characterization can be regarded as restricted to pairs that are close to the diagonal, where the first-order Taylor expansion of $\Phi_b(x)$ around $x = b$ is revealed. In order to test and expand these results, in *Experiment III* we measure the perceptual shift produced by surrounds in pairs that are further away from the diagonal, and report this shift in the perceptual coordinates. The obtained matches are consistent with the first-order expansion of the function $\Phi_b(x)$ found earlier, and allows us to extend the description to more dissimilar surrounds. More importantly, the experimental data confirm the assumption that, in the perceptual coordinates, the shift is homogeneous in color space, and isotropic among cardinal axes.

Below we list the hypothesis under which we construct the geometry of color space.

1. *The manifold of percepts is Riemannian*, so that the distance function d can be written

in terms of a metric tensor J . This hypothesis is implicit in Eqs. 3-7. The Riemannian assumption was first introduced by von Helmholtz (1892) and Schrödinger (1920), later discussed by Silberstein (1943), Stiles (1946), Resnikoff (1974), and da Fonseca da Fonseca and Samengo (2016, 2018), and is supported by the experimental observation that discrimination thresholds conform an ellipse around the reference color (MacAdam, 1944; Krauskopf and Gegenfurtner, 1992), so local distances can be approximated by a quadratic form.

2. *The metric tensor is decomposable as a direct sum in the isoluminant coordinates $x_1 = S$ and $x_2 = L - M$.* This hypothesis is implicit in Eqs. 4-7, and yields

$$d\ell^2 = J_{11}(x_1) dx_1^2 + J_{22}(x_2) dx_2^2, \quad (14)$$

as shown by Krauskopf and Gegenfurtner (1992). Therefore, a coordinate system exists (the *perceptual coordinates*) in which the distance between uniform representatives is Euclidean (Sect. 2.4).

3. *The space of percepts is complete*, such that for any pair of points $\mathbf{x}^\alpha, \mathbf{x}^\beta$, a geodesic $\gamma_{\mathbf{x}^\alpha \rightarrow \mathbf{x}^\beta}$ joining them exists such that $d(\mathbf{x}^\alpha, \mathbf{x}^\beta) = \text{length}(\gamma_{\mathbf{x}^\alpha \rightarrow \mathbf{x}^\beta})$. In particular, the separability of the isoluminant plane implies that the lines defined by the cardinal axes \mathbf{e}^1 and \mathbf{e}^2 are geodesics.

One of the central hypotheses of this paper is that, in the perceptual coordinates, the effect of the surround has rotational symmetry. More precisely, the function $\Phi_{\mathbf{b}}(\mathbf{x})$ is assumed to comply with two other requirements:

4. *The radial hypothesis:* If $\mathbf{x}^\alpha \parallel \mathbf{b}^\alpha \sim \mathbf{x}^\beta \parallel \mathbf{b}^\beta$, and $\mathbf{x}^\alpha, \mathbf{b}^\alpha$ and \mathbf{b}^β lie all on the same cardinal axis (either $\hat{\mathbf{e}}^1$ or $\hat{\mathbf{e}}^2$), the matched color \mathbf{x}^β also lies on the same axis. Evidence for this symmetry is discussed in *Experiment III*. So far, this hypothesis was formulated for the cardinal axis of the cone contrast coordinates. To make the statement more general, we observe that the conjecture suggests that the displacement produced by $\Phi_{\mathbf{b}}(\mathbf{x})$ acts along the line connecting the stimulus and the surround, such that for fixed \mathbf{b} , the vector field of displacements induced by $\Phi_{\mathbf{b}}(\mathbf{x})$ is radial and centered in \mathbf{b} . Graphically, in the vector fields of Fig. 4, arrows are parallel to the line joining \mathbf{b} and \mathbf{x} . In Riemannian geometries, the line connecting two points is generalized to a geodesic (Fig. 4A), so the precise formulation of the radial hypothesis reads: For fixed \mathbf{b} and viewed as a function of \mathbf{x} , the uniform representative $\Phi_{\mathbf{b}}(\mathbf{x})$ lies along the geodesic $\gamma_{\mathbf{b} \rightarrow \mathbf{x}}$ that starts from

\mathbf{b} and passes through \mathbf{x} . Moreover, if t is an arc-length affine parameter for $\gamma_{\mathbf{b} \rightarrow \mathbf{x}}(t)$, a scalar function $t(\mathbf{x}, \mathbf{b})$ exists, such that the uniform representative can be written as $\Phi_{\mathbf{b}}(\mathbf{x}) = \gamma_{\mathbf{b} \rightarrow \mathbf{x}}[t(\mathbf{x}, \mathbf{b})]$.

5. *Isotropy and homogeneity*: Color space is assumed to contain no privileged stimuli or directions, at least, when dealing with points that are far from the borders of the gamut (stimuli that are maximally saturated). Evidence for this hypothesis is provided by *Experiments II* and *III*. The core assumption is that the perceptual shift produced by a surround \mathbf{b} on a stimulus \mathbf{s} only depends on the distance $d(\mathbf{b}, \mathbf{x})$, that is, $t(\mathbf{x}, \mathbf{b}) = t[d(\mathbf{x}, \mathbf{b})]$. The perceptual coordinates are defined so as to ensure that equi-distant classes cross the diagonal in equi-distant points. Yet, from the definition of perceptual coordinates alone, there is no restriction on the shape of classes. The isotropy and homogeneity hypothesis implies that, when viewed in the perceptual coordinates, all the classes have the same shape, and only differ from one another in a rigid translation, as in all the examples of Fig. 3.

In the perceptual coordinates, the metric tensor reduces to the unit matrix, so all geodesics become straight lines, along which components can be summed and multiplied. In particular, the separability of the metric tensor (hypothesis 2) implies that the lines along the cardinal axes $\hat{\mathbf{e}}^1$ and $\hat{\mathbf{e}}^2$ are geodesics. In the perceptual coordinates, the mapping $\Phi_{\mathbf{b}}(\mathbf{x})$ can be written as

$$\Phi_{\mathbf{b}}(\mathbf{x}) = \gamma_{\mathbf{b} \rightarrow \mathbf{x}}\{t[d(\mathbf{x}, \mathbf{b})]\} = \mathbf{b} + t[d(\mathbf{b}, \mathbf{x})] \hat{\mathbf{u}}, \quad \text{with } \hat{\mathbf{u}} = \frac{\mathbf{x} - \mathbf{b}}{d(\mathbf{b}, \mathbf{x})}. \quad (15)$$

That is, in the perceptual coordinates, the color shift induced by the surround is radial, it is centered at the surround \mathbf{b} and is of magnitude $t[d(\mathbf{x}, \mathbf{b})]$ along the direction $\hat{\mathbf{u}}$ that connects \mathbf{b} and \mathbf{x} . If the surround exerts no influence (Fig. 3A) then $\Phi_{\mathbf{b}}(\mathbf{x}) = \mathbf{x}$, which necessarily implies that $t(d) = d$.

The effect of the surround is taken to be *repulsive* if $t(d) > d$ (the surround repels the stimuli, so that the uniform representative of a given stimulus is further away from the surround than the original stimulus), and *attractive* otherwise, that is, if $t(d) < d$.

3.3 Experiment I: Discrimination thresholds for $B = T$

Experiment I is used to find the perceptual coordinates of each observer, that is, the coordinates in which the discrimination thresholds around each color are constant and isotropic throughout color space. As explained in Sect.2.4, the derivation of the perceptual coordinates requires

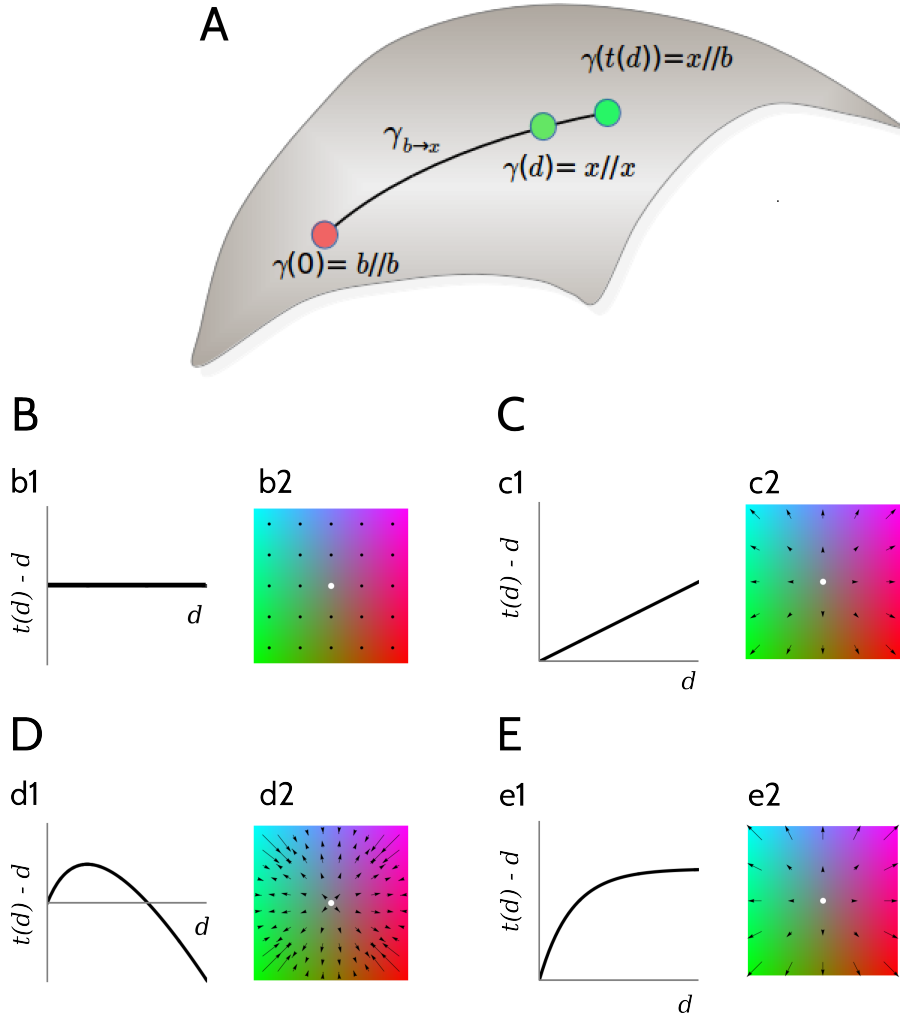


Figure 4: **Radially symmetric induction.** A: Hypothesis 4 and 5 state that when color x is surrounded by color b , the perceived sensation is chromatically equal to that of a uniform representative that lies along the geodesic $\gamma_{b \rightarrow x}$, displaced from x in an amount $t(d) - d$. The space \mathcal{P} contains all uniform representatives. In this example, the surround exerts a repulsive effect, since the $\gamma_{b \rightarrow x}[t(d)]$ is longer than $\gamma_{b \rightarrow x}(d)$. B-E: Four different examples of the shifts $t(d) - d$, corresponding to the classes of equivalence of Fig. 3. B: $t(d) = d$ (b1), and the vector field centered at the surround (white disk) vanishes in all the points of color space (b2). C: $t(d) \propto d$, with a proportionality factor different from unity. The vector field is linear. For $x = b$ the surround does not alter the perceived stimulus, but otherwise, the effect is radial, repulsive, and proportional to the distance between x and b . D: $t(d) \propto \ln(1 + d/\lambda)$, for some characteristic distance λ . The effect of the surround is initially repulsive, vanishes at $d = \lambda$, and then reverts to attractive. In E, $t(d) - d \propto [1 - \exp(-d/\lambda)]$, so the displacement is always repulsive, and tends to a constant value for large distances.

the knowledge of the metric tensor $J(x)$ of the submanifold of uniform representatives (Eqs. 6 and 7). We work with fixed luminosity, that is, $L + M = \text{const.}$ (Derrington et al., 1984). In order to estimate $J(x)$ in a 2-dimensional space, thresholds should be measured in at least

3 directions, so as to fit the 3 independent numbers that define the 2×2 quadratic form. As summarized by Hypothesis 2 above, Krauskopf and Gegenfurtner (1992) established that in the space $(x_1, x_2) = (S, L - M)$ defined by the cone contrasts, discrimination thresholds are described by diagonal quadratic forms. The ellipses, hence, are always elongated along the coordinate axes \hat{e}^1 and \hat{e}^2 . Moreover, their study also showed that the elongation of the ellipses along the \hat{e}^1 direction varied approximately linearly with x_1 , and bared no significant dependence on x_2 . The elongation along the \hat{e}^2 direction was shown to be approximately constant. These results can be used to greatly reduce the time required to measure the discrimination thresholds: It suffices to sample the thresholds around colors \mathbf{x} that lie along the cardinal axes, testing displaced colors $\mathbf{x} + \varepsilon_I \hat{e}$ that also lie along the same axis. The colors \mathbf{x} tested here are displayed in Fig. 1C.

We now deduce how the diagonal terms J_{ii} are obtained from the measured discrimination thresholds. For each uniform representative $\mathbf{x} \parallel \mathbf{x}$ sampled along the i -th coordinate axis ($i \in \{1, 2\}$), we determine the minimal displacement $\varepsilon_I(\mathbf{x}, \hat{e}^i)$ along the same direction \hat{e}^i , so that $\mathbf{x} + \varepsilon_I(\mathbf{x}, \hat{e}^i) \hat{e}^i \parallel \mathbf{x}$ be first distinguishable from $\mathbf{x} \parallel \mathbf{x}$. The sub-index “ I ” in ε_I indicates a threshold obtained with *Experiment I* (a different threshold is defined in *Experiment II*). Notice that in the uniform representative $\mathbf{x} \parallel \mathbf{x}$ the stimulus cannot be differentiated from the surround (Fig. 1A, left, right and upper patches), and the goal of the task is to determine the minimal value of $\varepsilon_I(\mathbf{x}, \hat{e}^i)$ required to detect the patch of chromaticity $\mathbf{x} + \varepsilon_I(\mathbf{x}, \hat{e}^i) \hat{e}^i$ against the surround \mathbf{x} (Fig. 1A, lower patch).

Defining the unit of distance in color space as that corresponding to the the just noticeable difference (Sect. 2.3.1), and making use of the assumption that distances derive from a diagonal metric tensor J ,

$$\begin{aligned}
1 &= d[\mathbf{x} \parallel \mathbf{x}, \mathbf{x} + \varepsilon_I(\mathbf{x}, \hat{e}^i) \hat{e}^i \parallel \mathbf{x}] \\
&= d\{\mathbf{x}, \Phi_{\mathbf{x}}[\mathbf{x} + \varepsilon_I(\mathbf{x}, \hat{e}^i) \hat{e}^i]\} \\
&= \text{Length of the geodesic } \gamma(t \{d[\mathbf{x}, \mathbf{x} + \varepsilon_I(\mathbf{x}, \hat{e}^i) \hat{e}^i]\}) \\
&= |t \{d[\mathbf{x}, \mathbf{x} + \varepsilon_I(\mathbf{x}, \hat{e}^i)]\}| \\
&\approx |t'(0) \sqrt{J_{ii}(\mathbf{x})} \varepsilon_I(\mathbf{x}, \hat{e}^i)|
\end{aligned} \tag{16}$$

Two factors determine the length $\varepsilon_I(\mathbf{x}, \hat{e}^i)$ corresponding to the just noticeable difference: The metric J , and the derivative $t'(d)$. The metric defines how distances are quantified in each point of color space and along each direction, and appears in any Riemmanian space. The derivative is a special ingredient that appears in our case, due to the fact that we are comparing classes (or equivalently, uniform representatives) and not just stimuli. The derivative quantifies the

displacement induced by the surround. If the surround exerts no influence (horizontal classes in Fig. 3A), then the derivative is equal to unity, since $\Phi_b(\mathbf{x}) = \mathbf{x}$ and $t(d) = d$. If the surround exerts a repulsive effect, the derivative is larger than unity. This case is illustrated in Fig. 3, where the contour lines have positive slope when crossing the diagonal. Repulsive surrounds increase the distance. Alternatively, to reach the same perceptual distance, a smaller threshold suffices. An attractive surround, instead, corresponds to $t'(d) < 1$.

Solving Eq. 16 for J_{ii} ,

$$J_{ii}(\mathbf{x}) = \left[\frac{1}{t'(0) \varepsilon_I(\mathbf{x}, \hat{\mathbf{e}}^i)} \right]^2. \quad (17)$$

This equation allows us to find the diagonal terms J_{ii} of the metric tensor from the measured thresholds $\varepsilon_I(\mathbf{x}, \hat{\mathbf{e}}^i)$, up to a multiplicative factor $t'(0)$. Figures 5A and C show the measured thresholds. Along the x_1 axis, thresholds increased roughly linearly with x_1 , with some subject-to-subject variability. Thresholds varied across subjects up to a factor of 3. Along the x_2 axis, thresholds showed a non monotonic behavior, with a minimum around $x_2 = 0$, which corresponds to the reference gray. Although there was a certain subject-to-subject variability, all observers showed evidence of the minimum. For each fixed subject, the modulation of thresholds was significantly smaller than along the S axis, with the maximal and minimal threshold of each observer differing in less than 50% of the minimal threshold. Hence, confirming the result of Krauskopf and Gegenfurtner (1992), thresholds along the $\hat{\mathbf{e}}^1$ direction vary more pronouncedly than along the $\hat{\mathbf{e}}^2$ direction. Yet, our data reveal that they do not remain strictly constant along the $\hat{\mathbf{e}}^2$ directions, since the mild non-monotonic behavior was found to be significant.

The threshold $\varepsilon_I(\mathbf{x}, \hat{\mathbf{e}}^i)$ is the change in chromaticity required for a stimulus to be discriminated from its surround with a fixed precision (Sect. 2.3.1). In Fig. 5E, this increment is the vertical displacement between a pair $\mathbf{x} \parallel \mathbf{x}$ on the diagonal, and a point $\mathbf{x} + \varepsilon_I(\mathbf{x}, \hat{\mathbf{e}}^i) \hat{\mathbf{e}}^i \parallel \mathbf{x}$ sitting right above (or below) the former, on the equivalence class at distance 1 from that of $\mathbf{x} \parallel \mathbf{x}$. If Fig. 5E were depicted in cone coordinates or in any other color space that had not been chosen to reflect perceptual distances, different triplets of yellow dots along the diagonal would appear to span different vertical height, since the vertical separation between just-noticeably-different classes (classes at distance 1) can be arbitrary. Finding the perceptual coordinates is equivalent to finding a representational system in which the vertical span of all triplets remain constant along the diagonal. In these coordinates, the classes intersect the diagonal at equi-distant intervals, as in Figs. 3 and 5E.

To define the perceptual coordinates along the axes $\hat{\mathbf{e}}^1$ and $\hat{\mathbf{e}}^2$, the square root of the diagonal

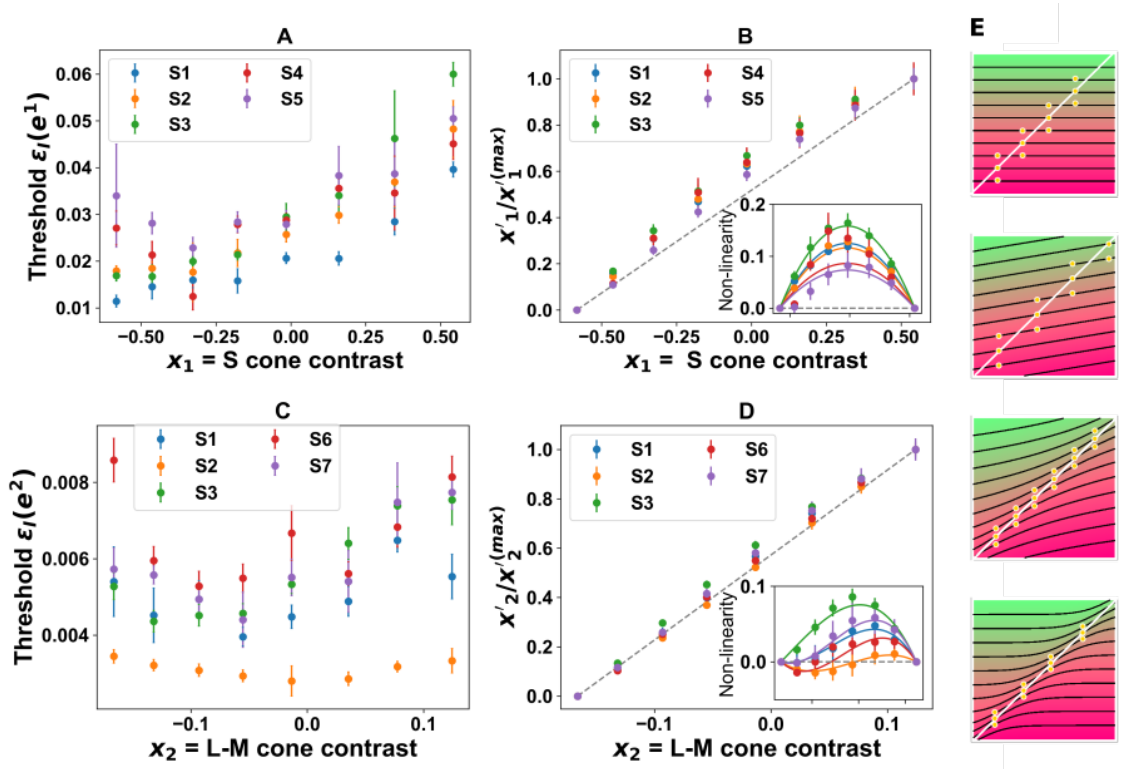


Figure 5: **Discrimination thresholds when the target and the surround chromaticities coincide.** A and C: Discrimination thresholds for the x_1 (A) and x_2 (C) cone contrast coordinates. Different observers displayed in different colors. B and D: perceptual coordinates $x'_1/x'_1(\max)$ (B) and $x'_2/x'_2(\max)$ (D) as a function of the cone contrasts. The normalizing factors $x'_i(\max)$ are the maximal perceptual coordinate obtained for each subject, and were used to scale the data in order to compare different observers, which would otherwise produce perceptual coordinates spanning intervals of different lengths. Insets: Deviations from the linear mapping. Each data point is obtained from the fit of Eq. 1, and error bars are the expected errors of the fit. Parameters of the optimal fits are given in Table 1. E: The measured thresholds represent the vertical displacement between a pair $x \parallel x$ on the diagonal (yellow dot), and another pair sitting right above, or just below, on a class of equivalence that is at perceptual distance 1 from that of $x \parallel x$.

elements of the metric have to be integrated (Eq. 5). To this aim, an analytic expression of $J^{1/2}(\mathbf{x})$ is needed. We propose a polynomial function

$$|t'(0)| \sqrt{J_{ii}(x_i)} = \frac{1}{\epsilon_I(\mathbf{x}, \hat{e}^i)} = \sum_{j=0}^n \alpha_j x_i^j, \quad (18)$$

and fitted the coefficients α_j to the data. The order n of the polynomial was chosen as the lowest that still accounted for the data with p -values above 0.01. Along the \hat{e}^1 axis, a straight line ($n = 1$) suffices, whereas the \hat{e}^2 axis requires to go up to a quadratic expression ($n = 2$). Table 1 of the Appendix contains the fitted parameters.

Along the \hat{e}^1 direction, the variability of the coefficients fitted for different observers indicated inter-individual differences, since a single set of coefficients α_j could not account for the metric tensor of different subjects. The p -value for the hypothesis that a single α_0 could be used for the 5 subjects was 10^{-8} , and for a single α_1 was $6 \cdot 10^{-3}$. Along the \hat{e}^2 direction, the individual differences were significant in the constant (p -value below 10^{-10}) and linear coefficients (p -value $2 \cdot 10^{-7}$), but not in the quadratic ones (p -value = 0.68).

Once an analytic expression has been obtained for the diagonal elements of the metric, the perceptual coordinates along the cardinal axes can be calculated by integration (Eqs. 6 and 7), except for the yet unknown factor $|t'(0)|$. In Figs. 5B and D, the normalized perceptual coordinates x'_1 and x'_2 are shown as a function of the corresponding cone contrasts x_1 and x_2 . The insets display the deviation from a linear mapping, together with the quadratic or cubic analytical expressions obtained by integrating Eq. 18 (same parameters as in Table 1). Importantly for what follows, in the perceptual coordinates, the distance between two colors \mathbf{x}' and \mathbf{y}' is calculated with the Euclidean formula. If the two colors lie along the cardinal axis \hat{e}^i , then $d(\mathbf{x}'\hat{e}^i, \mathbf{y}'\hat{e}^i) = |x'_i - y'_i|$.

3.4 Experiment II: Discrimination Thresholds for $B \neq T$

Experiment II involved the same discrimination task as *Experiment I*, but with a surround \mathbf{b} that was different from the tested stimuli. Since the discrimination threshold depends on the surround, we use the notation $\varepsilon_{II}(\mathbf{x}, \mathbf{b}, \hat{e}^i)$. *Experiment II* reduces to *Experiment I* when $\mathbf{b} = \mathbf{x}$, that is, $\varepsilon_{II}(\mathbf{x}, \mathbf{x}, \hat{e}^i) \equiv \varepsilon_I(\mathbf{x}, \hat{e}^i)$.

In *Experiment II*,

$$\begin{aligned} 1 &= d[\mathbf{x} \parallel \mathbf{b}, \mathbf{x} + \varepsilon_{II}(\mathbf{x}, \mathbf{b}, \hat{e}^i)\hat{e}^i \parallel \mathbf{b}] \\ &= d\{\Phi_{\mathbf{b}}(\mathbf{x}), \Phi_{\mathbf{b}}[\mathbf{x} + \varepsilon_{II}(\mathbf{x}, \mathbf{b}, \hat{e}^i)\hat{e}^i]\}, \end{aligned} \quad (19)$$

where the second line derives from the hypothesis that distances between two pairs remain invariant if any of the pairs is replaced by another member of its own class, in particular, the uniform representative. Since \mathbf{b} , \mathbf{x} and $\mathbf{x} + \varepsilon_{II}(\mathbf{x}, \mathbf{b}, \hat{e}^i)\hat{e}^i$ lie all three on the same cardinal axis,

$$d\{\Phi_{\mathbf{b}}(\mathbf{x}), \Phi_{\mathbf{b}}[\mathbf{x} + \varepsilon_{II}(\mathbf{x}, \mathbf{b}, \hat{e}^i)\hat{e}^i]\} = |d[\Phi_{\mathbf{b}}(\mathbf{x} + \varepsilon_{II}(\mathbf{x}, \mathbf{b}, \hat{e}^i)\hat{e}^i), \mathbf{b}] - d[\Phi_{\mathbf{b}}(\mathbf{x}), \mathbf{b}]|.$$

Replacing this result in Eq. 19,

$$\begin{aligned} 1 &= |t \{d[\mathbf{x} + \varepsilon_{II}(\mathbf{x}, \mathbf{b}, \hat{\mathbf{e}}^i) \hat{\mathbf{e}}^i, \mathbf{b}]\} - t[d(\mathbf{x}, \mathbf{b})]| \\ &\approx |t'[d(\mathbf{x}, \mathbf{b})] \sqrt{J_{ii}(\mathbf{x})} \varepsilon_{II}(\mathbf{x}, \mathbf{b}, \hat{\mathbf{e}}^i)| \end{aligned} \quad (20)$$

Since J_{ii} is known from Experiment I, we can use Eq. 17 to get

$$\varepsilon_{II}(\mathbf{x}, \mathbf{b}, \hat{\mathbf{e}}^i) = \varepsilon_I(\mathbf{x}, \hat{\mathbf{e}}^i) \left| \frac{t'(0)}{t'[d(\mathbf{x}, \mathbf{b})]} \right|. \quad (21)$$

Note that, as $t(d)$ is an arc length, the derivative $t'(d)$ is an invariant quantity - that is, independent of the coordinates. Therefore, although each threshold varies with the choice of coordinates, their ratio does not.

When the surround coincides with the stimulus, we get $\varepsilon_I = \varepsilon_{II}$. As the surround \mathbf{b} is moved away from the stimulus \mathbf{x} , the distance $d(\mathbf{x}, \mathbf{b})$ increases. The threshold ε_{II} may then either increase or decrease from ε_I , depending on whether the absolute value of the slope of $t(d)$ is larger or smaller than that of $t(0)$. Therefore, by measuring the thresholds ε_{II} for different surrounds, the derivative of $t(d)$ is revealed. Yet, this reasoning is only valid if the *isotropy and homogeneity hypothesis* proposed above (number 5 in Sect. 3.2) indeed holds, namely, the assumption that the perceptual shift induced by the surround only depends on the distance $d(\mathbf{x}, \mathbf{b})$. Therefore, before characterizing the shape of $t(d)$, we first use *Experiment II* to assess the validity of this hypothesis. To do so, we demonstrate that, in the perceptual coordinates, the dependence of the thresholds $\varepsilon_{II}(\mathbf{x}, \mathbf{b}, \hat{\mathbf{e}}^i)$ with \mathbf{b} and with \mathbf{x} can be entirely written in terms of the distance $|x'_i - b'_i|$.

The first step is to describe the dependence of the thresholds on the surround in the cone contrast coordinates. In Fig. 6, we see the variation of the thresholds from those obtained in *Experiment I* of a given subject as a function of the difference $x_i - b_i$. As reported by Krauskopf and Gegenfurtner (1992), the thresholds are minimal for $\mathbf{b} = \mathbf{x}$, and increase as the surround differs from the stimulus. This non-monotonic behavior refutes the hypothesis that classes be linear functions of the stimulus, as proposed by Resnikoff (1974). It then becomes important to characterize the variation. In *Experiment II*, the surround is always relatively close to the stimulus, so an expansion of $\varepsilon_{II}(\mathbf{x}, \mathbf{b}, \hat{\mathbf{e}}^i)$ around $\mathbf{b} = \mathbf{x}$ can be used to describe the measured thresholds.

If, as assumed in this paper, the function t depends on the coordinates through the distance d , the first-order of the Taylor expansion of t' must include the term $|x_i - b_i|$. Alternatively, if

Hypotheses 4 and 5 do not hold, thresholds would be expected to vary smoothly with the coordinates, in which case, a polynomial would provide a reasonable description of the dependence. We therefore compare two models containing the same number of parameters:

$$\text{Model 1 : } \varepsilon_{II}(\mathbf{x}, \mathbf{b}, \hat{\mathbf{e}}^i) - \varepsilon_I(\mathbf{b}, \hat{\mathbf{e}}^i) \approx \gamma_0 + \gamma_1(x_i - b_i) + \gamma_2(x_i - b_i)^2 \quad (22)$$

$$\text{Model 2 : } \varepsilon_{II}(\mathbf{x}, \mathbf{b}, \hat{\mathbf{e}}^i) - \varepsilon_I(\mathbf{b}, \hat{\mathbf{e}}^i) \approx \gamma_0 + \gamma_1(x_i - b_i) + \gamma_2|x_i - b_i| \quad (23)$$

The first model assumes that $\varepsilon_{II}(\mathbf{x}, \mathbf{b}, \hat{\mathbf{e}}^i)$ has a continuous derivative at $b_i = x_i$, and is able to describe the quadratic departure from linearity. The second model allows for the possibility of a discontinuous derivative, and for the ascending and the descending linear portions to have different slopes. It cannot, however, describe quadratic effects.

In Fig. 6, we compare the performance of the two proposals in fitting the measured thresholds.

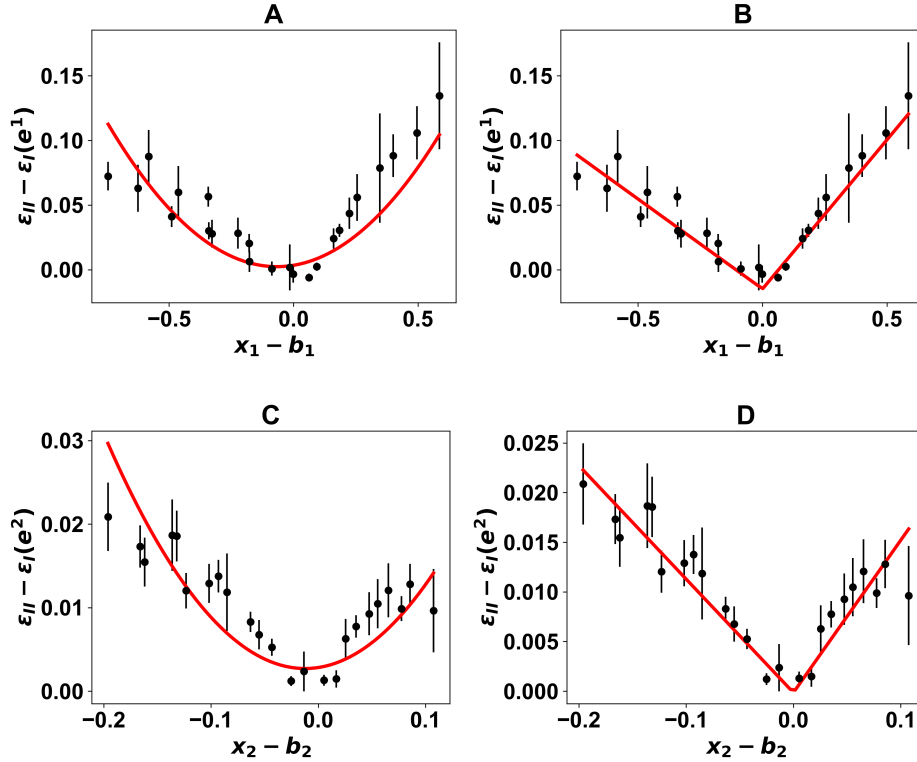


Figure 6: **Performance of models 1 and 2 in describing measured thresholds $\varepsilon_{II}(\mathbf{x}, \mathbf{b}, \hat{\mathbf{e}}^i)$.** Thresholds were measured for observer S2, and are shown as a function of $x_i - b_i$. Data points are obtained from the fit of Eq. 1, and error bars are the expected error of the fit. Red line: fitted model. A and C: Model 1 (Eq. 22). B and D: Model 2 (Eq. 23). A and B: Discrimination thresholds measured along $\hat{\mathbf{e}}^1$. C and D: Along $\hat{\mathbf{e}}^2$.

The fitted coefficients γ_0 , γ_1 and γ_2 are reported in Tables 2 and 3 of the Appendix. The constant term γ_0 is of the order of the experimental error of the measurements, confirming that when the stimulus and the surround coincide, ε_{II} indeed reduces to ε_I .

Each fit produces a χ^2 value quantifying the goodness of the fit for each subject and axis, and although there are small differences among conditions, the mean χ^2 -value obtained for Model 2 (averaged across subjects and axes) is half the value obtained for Model 1. Accordingly, the mean p -value obtained for the hypothesis that the data be generated with Model 2 is twice as large as with Model 1. These results imply that the data is better explained by Model 2, and a discontinuous derivative is to be expected at $\mathbf{b} = \mathbf{x}$. Moreover, the fact that γ_1 is typically significantly different from zero indicates that the ascending and the descending linear portions of Model 2 have different slopes.

To determine whether the hypothesis of homogeneity and isotropy is justified, we now transform \mathbf{x} , \mathbf{b} and ε_{II} to the perceptual coordinates, using Eqs. 6 and 7 and the metric tensor J_{ii} obtained with *Experiment I*. We emphasize that no data of *Experiment II* is used to fit the parameters of the transformation. Although we still lack the multiplicative constant $|t'(0)|$, we can nevertheless assess whether, in these coordinates, $\varepsilon'_{II}(\mathbf{x}', \mathbf{b}', \hat{\mathbf{e}}^i)$ indeed depends only on the difference $|x'_i - b'_i|$. If it does, the transformation should suffice to eliminate the asymmetry in the slopes of the descending and ascending portions of Model 2. Equivalently, when ε'_{II} (measured for a single subject with different stimuli \mathbf{x} , surrounds \mathbf{b} and axes $\hat{\mathbf{e}}^i$) is plotted as a function of $|x'_i - b'_i|$, a single straight line should be seen. This plot is displayed in column A of Fig. 7, for surrounds varying along the axis $\hat{\mathbf{e}}^1$ (top), $\hat{\mathbf{e}}^2$ (middle) and both axes together (bottom).

For comparison, we also show the same data points represented in other coordinate systems, to test whether the linear relation between $\varepsilon'_{II}(\mathbf{x}', \mathbf{b}', \hat{\mathbf{e}}^i)$ with $|x'_i - b'_i|$ indeed becomes more evident in the perceptual coordinates than in other coordinate systems. In column B, the data are plotted in cone contrast coordinates. Clearly, the points obtained for $b_i > x_i$ (circles) define a different slope from that for $b_i < x_i$ (squares). Moreover, the slopes along the axes $\hat{\mathbf{e}}^1$ and $\hat{\mathbf{e}}^2$ are markedly different (bottom row), and so are the total ranges of the data. As a consequence, the amount of dispersion is larger in the plots of column B than in column A. The χ^2 -values obtained from linear fits in column B are more than three times larger than those in column A, meaning that the data are more in line with the *Homogeneity and isotropy hypothesis* when plotted in the perceptual coordinates than in the cone contrasts.

In the cone contrast coordinate system, the origin $\mathbf{x} = \mathbf{0}$ is gray by convention. Columns

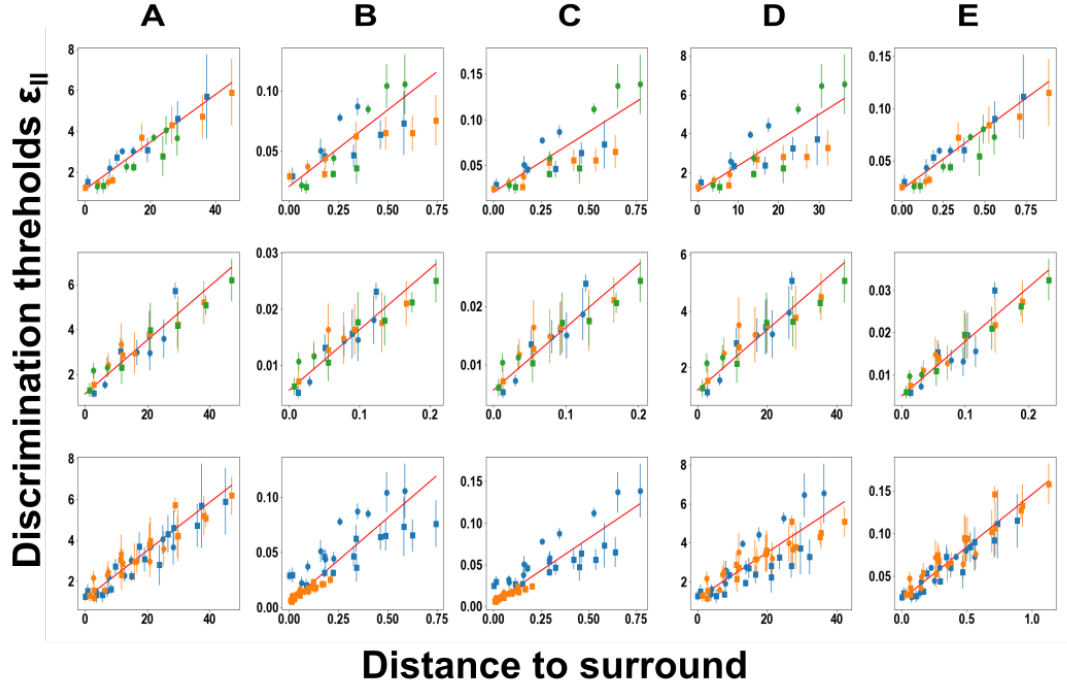


Figure 7: **Assessment of the validity of hypothesis 5.** Thresholds measured in *Experiment II* for subject S1 as a function of the distance between the surround and the stimulus. Circles: $b_i > x_i$. Squares: $b_i < x_i$. Each column represents a different choice of the system of coordinates in which thresholds, stimuli and surround are represented. A: perceptual coordinates defined with the data of Experiment I. Columns B, C, D: Other coordinates employed in the literature (see text), requiring no fitted parameters. Column E: Optimal coordinate system defined with a single fitted parameter. Top row: \mathbf{b} and \mathbf{x} lie along axis \hat{e}^1 . Green: $\mathbf{b} = (x_1, x_2) = (0.16, 0)$, blue: $\mathbf{b} = (0, 0)$, orange: $\mathbf{b} = (-0.24, 0)$. Middle row: axis \hat{e}^2 . Green: $\mathbf{b} = (0, 0)$, blue: $\mathbf{b} = (0, -0.03)$, orange: $\mathbf{b} = (0, 0.03)$. Bottom: both axes together. Blue data points: \hat{e}^1 . Orange: \hat{e}^2 .

C and D evaluate the performance of two additional coordinate systems, in which cone contrast is determined with respect to the chromatic surround in which the discrimination task was performed. Specifically, if the supra-index cc represents cone contrasts, in column C, the coordinates of both the stimulus and the surround are defined by the relation $x_i^{\text{new}} = x_i^{cc} / (b_i^{cc} + 1)$, so that changes in stimuli are represented by the relative contrast to the surround.

If ε_{II} depended only on the ratio x_i/b_i , Weber's law (Wyszecki and Stiles, 1982) would hold. In column D, the transformation is $x_i^{\text{new}} = x_i^{cc} / \varepsilon_I(\mathbf{b}, \hat{e}^i)^{cc}$, so that the threshold of the surround always corresponds to unity. If ε_{II} depended only on the ratio $\varepsilon_I(\mathbf{x}, \hat{e}^i) / \varepsilon_I(\mathbf{b}, \hat{e}^i)$, a modified version of Weber's law, formulated in terms of thresholds, would govern discriminability. The resulting average χ^2 values represent a three-fold (column C) and a two-fold (column D) increase with respect to the first column. Thus, again, the perceptual coordinates describe better

the linear relation.

While the first four models assessed coordinate systems that contained no free parameters, the last column was constructed by searching for the value of a free coefficient α , obtained from a fit to the data, that produced the mapping $x_i^{\text{new}} = x_i^{\text{cc}} + \frac{\alpha}{2}(x_i^{\text{cc}})^2$ with minimal χ^2 -value. The improvement, however, was only marginal, with a χ^2 -value that was only 6% smaller than that for the first coordinate system. The perceptual coordinates, hence, achieve almost the same performance as the ones of the last model without parameters determined from the data of *Experiment II*.

In Fig. 5E, discrimination thresholds are represented as the vertical distance between yellow dots. We could add additional dots to the figure, thereby extending the triplets to longer vertical sequences, unfolding both upwards and downwards, marking consecutive classes that always lie at perceptual distance 1 from their neighbors. The thresholds $\varepsilon_{II}(\mathbf{x}, \mathbf{b}, \hat{e}^i)$ would be represented by the vertical separation of consecutive dots. Linearly growing thresholds, as those of Fig. 7A, imply that classes become increasingly separated as we depart from the diagonal. Yet, in *Experiment II*, the range of colors was restricted by the gamut of the computer monitor, so the achievable chromatic difference between stimulus and surround was limited. Hence, the linear relation could only be confirmed for the limited range around the diagonal, where ε_{II} is well approximated by a linear function of its arguments. When defining the perceptual coordinates, we guaranteed that classes were equi-distant right on the diagonal. Yet, beyond the diagonal, in principle distances could vary. *Experiment II* showed that the separation $\varepsilon_{II}(\mathbf{x}, \mathbf{b}, \hat{e}^i)$ depended only on the distance $|x'_i - b'_i|$. Therefore, if the distance $|x'_i - b'_i|$ is changed in a fixed amount, the separation is always the same, irrespective of the individual values of x'_i and b'_i . At least in some region around the diagonal, the lines representing the classes are rigid translations one from each other. In this region, the results of *Experiment II* support the isotropy and homogeneity hypothesis.

The linear dependency of $\varepsilon_{II}(d)$ with d found in *Experiment II* restricts the set of feasible functions $t(d)$. For example, in the two upper panels of Fig. 5E, the separation between consecutive lines is constant, so the results of *Experiment II* discard these two options. The two lower panels correspond to cases in which $\varepsilon_{II}(d) - 1 \propto d$, for small d . Therefore, thus far, they both constitute possible candidate descriptions of the effect of the surround on the classes of equivalence. We now compare these options.

Let us first assume that the initial linear trend apparent in the data shown in Fig. 7 continues

also for larger distances. This hypothesis implies that ε_{II} is proportional to $1 + \lambda d(\mathbf{x}, \mathbf{b})$. It then follows that $t'(d)/t'(0) = (1 - \lambda d)^{-1}$, which in turn yields $t(d) = t'(0) \ln(1 + \lambda d)/\lambda$. The resulting displacement $t(d) - d$ is illustrated in panel *d1* of Fig. 4. The effect of the surround is initially repulsive, becomes neutral at an intermediate distance in which $t(d) = d$, and reverts to attractive for even larger distances (see the inversion of the arrows representing the vector field in panel *c2* of Fig. 3). Actually, $t(d)$ can even become negative. This behavior challenges our intuition in several ways, namely:

- Thresholds grow unbounded, implying that sufficiently distant surrounds preclude the discrimination of stimuli altogether, no matter how different.
- The displacement induced by the surround grows indefinitely for large distances. Therefore, the perceived color may differ from the presented one in an arbitrary amount, by simply displacing the surround far enough.
- The effect inverts its polarity (from repulsive to attractive) as the distance grows. The distance where the inversion takes place is singled out.
- Two different surrounds (one on each side of the neutral point) acting on the same stimulus may induce the same apparent color, even though intermediate surrounds produce different apparent colors.
- If the distance between the stimulus and the surround is sufficiently large, $t(d)$ vanishes. At that point, the stimulus becomes equal to the surround, producing a spatially uniform percept. At even larger distances, the perceived stimulus is on the negative side of the geodesic. In other words, a green stimulus surrounded by red can give rise to a red percept that is even more saturated than the surround.

In order to avoid these bizarre effects, thresholds should deviate from the linear behavior at large distances, decelerating. The simplest deviation from the linear hypothesis would be for thresholds to saturate after the initial linear growth. Such saturation can be modelled as $\varepsilon_{II}(d) \propto [1 + a \exp(-d/\lambda)]^{-1}$, as in panel *e1* of Fig. 4. The limited range in which *Experiment II* was performed (Fig. 7) does not show strong evidence of saturation. Yet, one can still test whether the thresholds of Fig. 7 can also be compatible with a sublinear trend. To this end, we compared the hypotheses that $t'(d) \propto (1 + d/\lambda)^{-1}$ (compatible with linear thresholds) and $t'(d) \propto 1 + ae^{-d/\lambda}$ (compatible with exponentially saturating thresholds). Slightly smaller χ^2 values were obtained for the exponential model. Even though the improvement in the fit

of *Experiment II* was only marginal, in the next section we describe *Experiment III* with the exponentially saturating model, thereby avoiding the unrealistic effects described above.

3.5 Experiment III: Asymmetric matching task

In the asymmetric matching task (Sect. 2.3.2), for each stimulus-surround pair $\mathbf{x}^\alpha \parallel \mathbf{b}^\alpha$ and surround \mathbf{b}^β the task of the observer was to find the stimulus \mathbf{x}^β that fulfills $\mathbf{x}^\alpha \parallel \mathbf{b}^\alpha \sim \mathbf{x}^\beta \parallel \mathbf{b}^\beta$, in other words, to report $\mathbf{x}^\beta = \Phi_{\mathbf{b}^\alpha \rightarrow \mathbf{b}^\beta}(\mathbf{x}^\alpha)$. Equation 10 implies that this condition is equivalent to

$$\Phi_{\mathbf{b}^\beta}(\mathbf{x}^\beta) = \Phi_{\mathbf{b}^\alpha}(\mathbf{x}^\alpha). \quad (24)$$

If the stimulus and the surround are both on the same cardinal axis $\hat{\mathbf{e}}^i$, Eq. 15 yields

$$\Phi_{\mathbf{b}}(\mathbf{x})|_i = \gamma \{t[d(\mathbf{x}, \mathbf{b})]\}_i = b_i + t[d(\mathbf{x}, \mathbf{b})] \text{Sgn}[x_i - b_i]. \quad (25)$$

If this condition is inserted in Eq. 24,

$$b_i^\beta + t[d(\mathbf{x}^\beta, \mathbf{b}^\beta)] \text{Sgn}[x_i^\beta - b_i^\beta] = b_i^\alpha + t[d(\mathbf{x}^\alpha, \mathbf{b}^\alpha)] \text{Sgn}[x_i^\alpha - b_i^\alpha].$$

In the perceptual coordinates, $d(\mathbf{x}, \mathbf{b}) = |x_i - b_i|$. Using this equality, and a few algebraic manipulations,

$$\left| [t(d^\beta) - d^\beta] - [t(d^\alpha) - d^\alpha] \text{Sgn}[x_i^\alpha - b_i^\alpha] \text{Sgn}[x_i^\beta - b_i^\beta] \right| = \left| x_i^\alpha - x_i^\beta \right| \quad (26)$$

Therefore, the perceptual shift $|x_i^\beta - x_i^\alpha|$ induced by the two surrounds only depends on the distances $d^\alpha = d(\mathbf{x}^\alpha, \mathbf{b}^\alpha)$ and $d^\beta = d(\mathbf{x}^\beta, \mathbf{b}^\beta)$ between each stimulus and its surround: As long as d^α and d^β remain constant, the shifts depend on none of the individual values $x_i^\alpha, x_i^\beta, b_i^\alpha$ or b_i^β , nor on the direction $\hat{\mathbf{e}}^i$. As a consequence, if shifts are plotted as a function of d^α and d^β , the set of data points should define a 2-dimensional manifold, no matter how many stimuli, surrounds and cardinal axes be included. Moreover, the 2-dimensional structure should only be evident in the perceptual coordinates, since in any other coordinate system, $d \neq |x_i - b_i|$, implying that Eq. 26 does not hold. In Fig. 8, the obtained graphs are displayed. Along each coordinate axes, the shifts define a 2-dimensional manifold, both in the cone contrast and the perceptual coordinates. If both axes are mixed, however, in the perceptual coordinates the collection of data points still lie on a 2-dimensional manifold, since the two sheets corresponding to the different axes coalesce. This is not the case in the cone contrast coordinates, since the sheet corresponding to $\hat{\mathbf{e}}_2$ is significantly closer to the origin than that of $\hat{\mathbf{e}}_1$. To quantify this difference, we estimated the dimension D of the manifold containing the data (Granata and

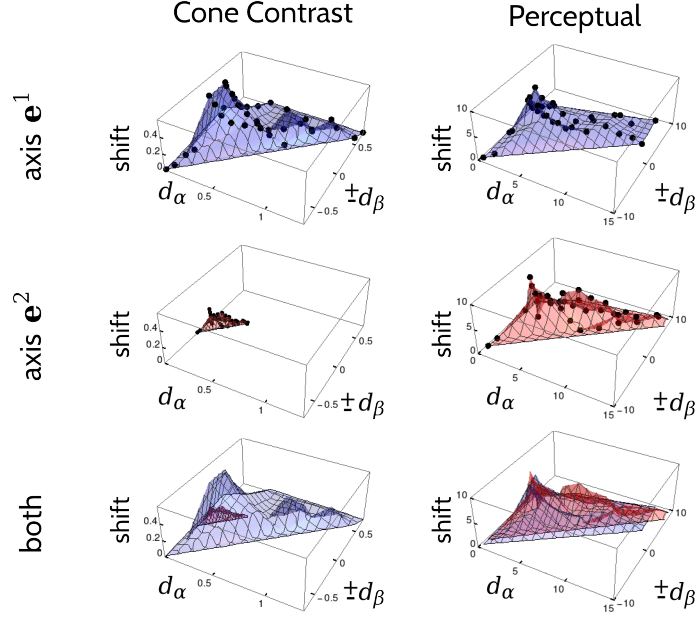


Figure 8: **Perceptual shifts induced by surrounds.** Shifts as a function of the distances $d^\alpha = |x_i^\alpha - b_i^\alpha|$ and $\pm d^\beta = \pm |x_i^\beta - b_i^\beta|$, for observer S3, along the axis \hat{e}^1 (top), \hat{e}^2 (middle) and both together (bottom), in cone contrast coordinates (left) and perceptual coordinates (right). The factor ± 1 multiplying d^β is defined by the product of Sign functions in Eq. 26. The measured data points appear in the top and middle panels, and the surface interpolates the measured values. In the lower panels, the two sheets are shown to coalesce in the perceptual coordinates, but not in the cone contrast.

Carnevale, 2016), obtaining $D = 2.11$ in the perceptual coordinates, and $D = 3.19$ in the cone contrast coordinates.

In order to test whether the exponential model provided a good description of the results of *Experiment III*, for each human observer we simulated a computational agent performing the same forced choice task. The agent decided in each trial which of the two candidate stimuli was most similar to the target, and did so according to their own idiosyncratic metric, as determined in *Experiment I*. This metric was used to represent the experiment in the perceptual coordinates. In these coordinates, the effect of the surround was modeled as $\Phi_b(\mathbf{x})|_i = x_i + \kappa \text{Sign}(x_i - b_i) [1 - \exp(-|x_i - b_i|/\lambda)]$. This functional form gives rise to an initial linear growth of $\epsilon_{II}(d)$, and an exponential saturation for long distances. For each target color \mathbf{x}^α presented on a surround \mathbf{b}^α and two candidate colors \mathbf{x}^p and \mathbf{x}^q on the surround \mathbf{b}^β , the agent had to decide whether $d[\Phi_{\mathbf{b}^\alpha}(\mathbf{x}^\alpha), \Phi_{\mathbf{b}^\beta}(\mathbf{x}^p)]$ was larger or smaller than $d[\Phi_{\mathbf{b}^\alpha}(\mathbf{x}^\alpha), \Phi_{\mathbf{b}^\beta}(\mathbf{x}^q)]$. Guided by the choices of the agent, the iterative procedure of the experiment produced the final $\mathbf{x}^\beta = \Phi_{\mathbf{b}^\alpha \rightarrow \mathbf{b}^\beta}(\mathbf{x}^\alpha)$. Since significant amounts of trial-to-trial variability were observed in the responses (Fig. 5), additive Gaussian noise, with zero mean and a variance

fitted for each subject, was included in the evaluation of the distances $d[\Phi_{b^\alpha}(x^\alpha), \Phi_{b^\beta}(x^p)]$ and $d[\Phi_{b^\alpha}(x^\alpha), \Phi_{b^\beta}(x^q)]$ computed by the simulated observers. The simulated responses were therefore also stochastic. The functional form proposed for $t(d)$ contains two free parameters, κ and λ . The fitting procedure was implemented with the python package *noisyopt* [Spall (1998), Mayer et al. (2016)], which handles noisy functions. A single exponential function and a single noise variance was fitted for each observer, for the three different pairs of surrounds on each axis, and for both axes. Figure 9 displays the resulting x^β values as a function of the target x^α for subject S3, on four different pairs of surrounds, two for each axis. Simulated matches

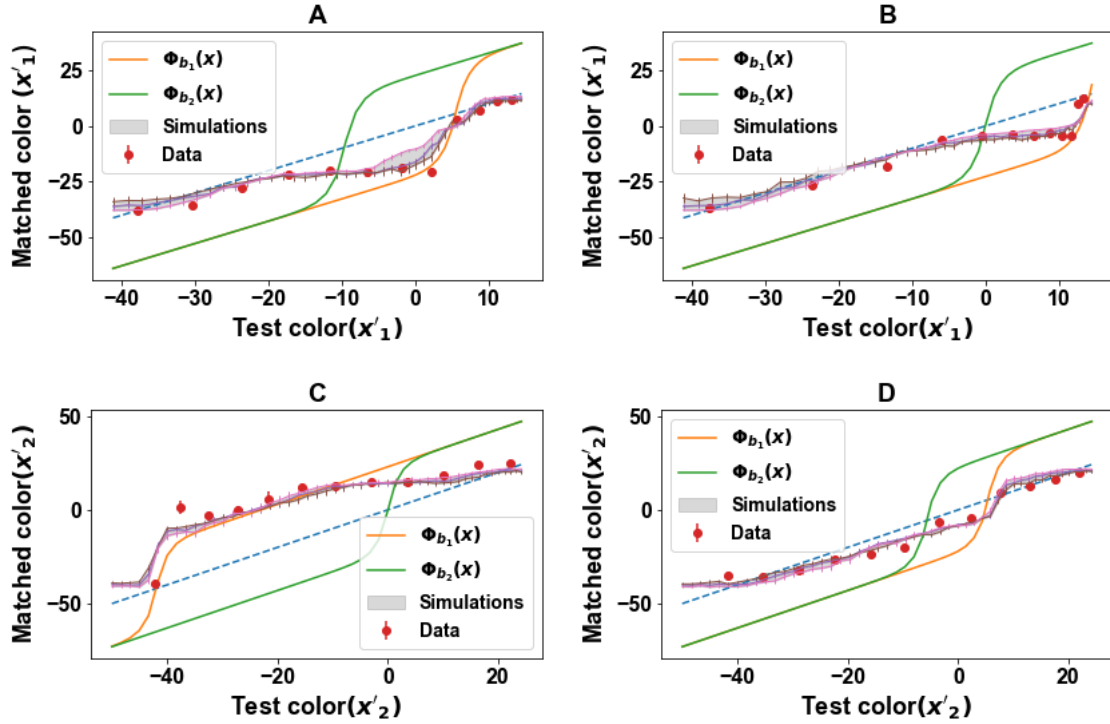


Figure 9: **Comparison between the measured and simulated data in Experiment III.** Matched color x^β as a function of the target color x^α (both axes in the perceptual coordinates) for observer S3. A and B: Asymmetric matching along the axis \hat{e}^1 . C and D: Asymmetric matching along the axis \hat{e}^2 . In the cone contrast coordinates, the two surrounds were $b^\alpha = (-0.35, 0)$ and $b^\beta = (0.25, 0)$ (A), $b^\alpha = (0, 0)$ and $b^\beta = (0.9, 0)$ (B); $b^\alpha = (0, 0)$ and $b^\beta = (0, -0.2)$ (C), $b^\alpha = (0, -0.03)$ and $b^\beta = (0, 0.03)$ (D). Red circles: experimental data. Violet line: Simulated results. Shaded areas: standard deviation of the simulated results. Blue dotted line: identity function, expected in the case in which the surround exerts no influence. Green and orange lines: mappings $\Phi_{b^\alpha}(x^\alpha)$ and $\Phi_{b^\beta}(x^\alpha)$ obtained from the fitted values of κ and λ of observer S3, indicating the uniform representatives of $x^\alpha \parallel b^\alpha$ and $x^\alpha \parallel b^\beta$, respectively. The perceptual shift induced by the surround becomes relevant in the interval of x^α values for which the two shifts (green and orange curves) are unequal, thereby producing a net unbalance.

may sometimes appear to be discontinuous (for example first data point in Fig. 9C). This behavior derives from the staircase procedure employed to approach the matched stimulus, since for some test colors, neither the human nor the simulated subjects can select colors that (in their subjective experience) are shifted by the induction of the surround outside the two offered options. The shift induced by the surround becomes significant in the interval of target x^α values in which the push/pull produced by one of the surrounds is not compensated by the other, that is, where the green and orange lines differ. The simulations reproduced qualitatively the measured data.

4 Discussion

This paper constructs a notion of distance from a Riemannian geometry in a perceptual space, such that the symmetries governing the mapping of sensory stimuli to percepts are most simply revealed. It does so in color space, as an example of a perceptual space in which the discriminability of neighboring stimuli does not depend linearly on notions of distance defined in terms of simple quantities derived from the physical stimulus. Our work embraces the conceptual framework first introduced by Resnikoff (1974), and recently reviewed by Provenzi (2020), in which color is understood as a property of classes of equivalence in the space of stimulus-surround pairs. This framework was based on the observation that colored surrounds modify the appearance of color stimuli. Our starting point was the assumption that, far away from the borders of color space, the perceptual effect of a given surround on a given stimulus is governed by a universal law. Here, “universal” means that a notion of distance $d(x_1 \parallel b_1, x_2 \parallel b_2)$ between classes exists, such that

$$\Phi_b(x) = \gamma_{b \rightarrow x} \{t[d(x, b)]\}, \quad (27)$$

where $\gamma_{b \rightarrow x}$ is the geodesic connecting b and x obtained from the postulated distance, and t some function that we still need to specify. Equation 27 is a strong assumption. If no symmetries are assumed, $\Phi_b(x)$ can be any transformation $\mathbb{R}^3 \times \mathbb{R}^3 \rightarrow \mathbb{R}^3$. Once Eq. 27 is imposed, the characterization of $\Phi_b(x)$ reduces to determining the function $t : \mathbb{R}^+ \rightarrow \mathbb{R}^+$, which is a much simpler object. If, in addition, the postulated distance derives from a metric tensor with zero curvature, then a system of coordinates exists, here called the *perceptual coordinates*, in which the perceptual distance is Euclidean. In this coordinate system, all the classes of equivalence have the same shape, and only differ from one another by a rigid translation. The freedom in the shape of $t(d)$ implies that there is freedom in the shape of a single class. Yet, once the manifold corresponding to a single class is known, all others are known too.

In this paper, we tested the hypothesis that the notion of distance required to model chromatic induction through Eq. 27 also governed the similarity of chromatic stimuli in terms of discrimination thresholds. If a single notion of distance is involved in a variety of experiments, one may suspect that the space of colors indeed possesses a natural geometry, accessible by many - if not all - the computations implicated in the transformation from input stimuli into behavioral responses. It therefore makes sense to study the geometry of color space, because such geometry is not idiosyncratic to specific tasks: It remains invariant throughout a variety of paradigms.

Previous work (Krauskopf and Gegenfurtner, 1992; da Fonseca and Samengo, 2016, 2018) had demonstrated that, when color was represented in the cone contrast coordinates, the principal axes of the discrimination ellipsoids were aligned with the coordinate axes. In these coordinates, the metric tensor is decomposable as a direct sum and therefore, has zero curvature. Since the curvature is an invariant property that does not depend on the coordinates, we concluded that the space of colors has zero curvature, and that the perceptual coordinates exist. Importantly, the transformation yielding the perceptual coordinates was significantly different for different observers, implying that no unique coordinate system exists that is perceptually uniform for all trichromats. This finding is in line with the subject-to-subject variability predicted by theoretical derivations in discrimination experiments (da Fonseca and Samengo, 2016), the population variability in color matching experiments (Stiles and Burch, 1959; Wyszecki and Fielder, 1971; Alfvén and Fairchild, 1997; Fairchild and Heckaman, 2013, 2016; Asano et al., 2016b,a), and experimental studies on chromatic memory (da Fonseca et al., 2019). It is also consistent with the recurrently failed attempts to define a unique coordinate system perceived as perceptually uniform by all observers.

The perceptual coordinates were defined solely from discrimination thresholds measured with a single fixed surround (*Experiment I*) and contain no parameters derived from discrimination or induction thresholds for other surrounds (*Experiments II and III*). These coordinates fixate the spacing between uniform representatives. In order to verify whether the homogeneity and isotropy hypotheses hold, we performed *Experiments II and III*. In *Experiment II*, we showed that, in the perceptual coordinates, the function $t'(|x_i - b_i|)$ was indeed able to describe discrimination experiments in which the stimulus differed from the surround, along both chromatic axes (Fig. 7). Importantly, in the perceptual coordinates, $|x_i - b_i|$ is the Euclidean distance. Other coordinate systems, instead, yielded data points that could not be well described by a universal law. These results were restricted to regions of color space in which x remained fairly close to b . Therefore, only the first order Taylor expansion of $t(d)$ could be obtained

from *Experiment II*. Only a restricted collection of surrounds was measured, due to the limited range of colors that can be produced by a computer monitor. Since discrimination thresholds grow as the chromatic distance between stimulus and surround increases, the range of discrimination experiments that can be performed with contrasting surround is limited. This limitation was overcome by *Experiment III*, in which a perceptual match, instead of a discrimination, was required from the observer. The results of the match, once again, were revealed to be more universal when displayed in the perceptual coordinates than in cone contrast coordinates (Fig. 8).

The larger range of distances explored in *Experiment III* allowed us to gather evidence about different candidate functions $1/t'(d)$. The results of *Experiment II* contradicted Resnikoff's conjecture of linear classes, and thereby, of thresholds that remained constant as the surround moved away from the stimulus. The hypothesis that follows in simplicity assumes that thresholds grow linearly with d . Yet, this assumption implies that $t(d)$ grows indefinitely in a logarithmic manner, which means that the shift $t(d) - d$ produced by the surround changes sign, a behavior that is counterintuitive. The simplest next alternative is that after an initial linear trend, thresholds decelerate, and do so sufficiently fast so as to force the perceptual shift $t(d) - d$ to saturate for large distances. One simple way to model this behavior is with thresholds that approached exponentially their upper bound. The comparison between these two options gave a slightly better result for the exponential model. This model was also able to reproduce the temporal sequence of choices of subjects, as illustrated in Fig. 9. We therefore conclude that the effect of surrounds on the perceived color of stimuli can be modeled with Eq. 27, with a notion of distance that is individually tailored for each observer, and characterized by the structure of just noticeable distances. The perceptual shift $t(d) - d$ could be well fitted by a simple law that saturated exponentially for large distances.

The universality entailed in Eq. 27 suggests that the same mechanism by which surround b_1 modifies the perceived color of stimulus x_1 is active when surround b_2 modifies the perceived color of stimulus x_2 . This mechanism is likely to be implemented by lateral or convergent feed-forward connections underlying modulatory interactions in visual neurons (Zeki, 1983; Schein and Desimone, 1990; Wachtler et al., 2003) and may be the same mechanism underlying perceptual shifts in different modalities (Klaume and Wachtler, 2015). If a single physiological mechanism is responsible for the induction observed in different regions of color space, then the perceptual coordinates are probably the substrate upon which the synaptic processes instantiating induction operate. This hypothesis would imply that the perceptual coordinates represent signals that actually exist in the brain, and not just a mathematical construct.

The conclusions supported by our experiments can only be claimed to hold *far away from the borders of color space*, since this is the region that could be tested with our computer monitor. Color space is confined into a cone included inside the positive portion of the 3-dimensional *SML* space, the borders of which are the maximally saturated colors. These colors cannot be generated with broadband stimuli as produced by computer displays. The existence of a border in color space blatantly contradicts the homogeneity hypothesis. We therefore take special care to limit the validity of our results, since color space cannot be homogeneous near its borders. As a consequence, the exponential model for the repulsive effect produced by surrounds cannot hold near maximally saturated stimuli, since it would push the perceived color outside the boundaries of color space. Maybe, close to the borders, chromatic induction diminishes. Physiologically, this would mean that when color-representing neurons are firing within a certain specific range (probably their maximal rates) the synaptic mechanisms mediating the chromatic induction produced by surrounds becomes negligible. Another possibility is that chromatic induction remains constant, but that the metric becomes singular near the borders. If thresholds tend to zero sufficiently fast as we approach saturated colors, in perceptual coordinates the border of color space would be pushed away to infinity. A third alternative would be that chromatic induction still holds at the border, so that perceived colors are indeed pushed outside the space generated by uniform representatives. This would imply that the assumption that all classes of equivalence contain a uniform representative breaks down at the borders of color space, and the most saturated colors from the perceptual point of view always correspond to cases of non-matching stimulus and surround. Experiments with saturated colors are required to differentiate these alternatives.

We conclude that the space of colors can be endowed with a notion of distance and a system of coordinates that transparently reveal the symmetry of perceptual effects. The notion of distance stems from discrimination experiments in which just-noticeable differences are used to define the metric tensor. We hope these results motivate similar attempts in other perceptual spaces and other sensory modalities, so that the generality of these results can be assessed.

Acknowledgments

This work was supported by the Agencia Nacional de Promoción de la Investigación, el Desarrollo Tecnológico y la Innovación, the Consejo Nacional de Investigaciones Científicas y Técnicas, the Comisión Nacional de Energía Atómica and the Universidad Nacional de Cuyo

of Argentina, and by the Bernstein Center for Computational Neuroscience Munich, Germany. The authors wish to thank the subjects that participated in the experiment, and to Sarah Theimer and Hongbin Wu for summoning volunteers and discussing previous versions of the behavioral paradigm.

Data availability

Experimental data can be found at https://gin.g-node.org/nicolas.vattuone/Perceptual_spaces_and_their_symmetries. DOI: 10.12751/g-node.5lyqp

Appendix

Table 1: Parameters of the linear and quadratic fits of $x'_i(x_i)$. The reported p -values represent the probability that data as extreme as the ones obtained in the experiment be generated with the fitted model.

| J_{11} | | | | J_{22} | | | | |
|----------|------------|-------------|------------|----------|-------------------|-------------------|-------------------|------------|
| Sub. | α_0 | α_1 | p -value | Sub. | $\alpha_0(.10^2)$ | $\alpha_1(.10^2)$ | $\alpha_2(.10^3)$ | p -value |
| S1 | 51 ± 3 | -47 ± 8 | 0.9962 | S1 | 2.14 ± 0.13 | -2.0 ± 0.4 | -1.7 ± 0.8 | 0.8826 |
| S2 | 39 ± 3 | -33 ± 6 | 0.9995 | S2 | 3.4 ± 0.2 | -0.55 ± 0.35 | -1.7 ± 0.8 | 0.9991 |
| S3 | 36 ± 2 | -42 ± 7 | 0.9933 | S3 | 1.85 ± 0.08 | -2.9 ± 0.3 | -0.94 ± 0.44 | 0.4808 |
| S4 | 38 ± 3 | -24 ± 7 | 0.2271 | S6 | 1.72 ± 0.08 | -1.1 ± 0.2 | -1.7 ± 0.5 | 0.5026 |
| S5 | 31 ± 2 | -17 ± 6 | 0.6555 | S7 | 1.89 ± 0.14 | -2.2 ± 0.4 | -2.0 ± 0.8 | 0.9901 |

Table 2: Fitted coefficients for Models 1 and 2 (Eqs. 22 and 23) for all measured subjects along the axis \hat{e}^1 .

| | Model 1 | | | Model 2 | | |
|----|--------------------|-------------------|-----------------|---------------------|------------------|-------------------|
| | γ_0 | γ_1 | γ_2 | γ_0 | γ_1 | γ_2 |
| S1 | 0.014 ± 0.004 | 0.058 ± 0.01 | 0.21 ± 0.04 | 0.001 ± 0.005 | 0.13 ± 0.02 | 0.053 ± 0.01 |
| S2 | 0.0034 ± 0.002 | 0.032 ± 0.009 | 0.24 ± 0.02 | -0.015 ± 0.003 | 0.18 ± 0.01 | 0.046 ± 0.009 |
| S3 | 0.0071 ± 0.004 | 0.047 ± 0.01 | 0.11 ± 0.03 | -0.0043 ± 0.005 | 0.087 ± 0.02 | 0.043 ± 0.009 |
| S4 | 0.0075 ± 0.003 | 0.019 ± 0.01 | 0.23 ± 0.03 | -0.0036 ± 0.004 | 0.13 ± 0.02 | 0.012 ± 0.01 |
| S5 | 0.0075 ± 0.003 | 0.055 ± 0.01 | 0.33 ± 0.03 | -0.012 ± 0.004 | 0.2 ± 0.02 | 0.054 ± 0.01 |

Table 3: Fitted coefficients for Models 1 and 2 (Eqs. 22 and 23) for all measured subjects along the axis \hat{e}^2 .

| | Model 1 | | | Model 2 | | |
|----|---------------------|-------------------|-----------------|-----------------------|-----------------|-------------------|
| | γ_0 | γ_1 | γ_2 | γ_0 | γ_1 | γ_2 |
| S1 | 0.0031 ± 0.0008 | 0.018 ± 0.02 | 0.73 ± 0.1 | $7.3e - 06 \pm 0.001$ | 0.13 ± 0.02 | 0.018 ± 0.01 |
| S2 | 0.0028 ± 0.0003 | 0.02 ± 0.007 | 0.8 ± 0.07 | -0.00015 ± 0.0004 | 0.13 ± 0.01 | 0.02 ± 0.007 |
| S3 | 0.0022 ± 0.0007 | 0.024 ± 0.009 | 0.69 ± 0.09 | -0.0011 ± 0.001 | 0.12 ± 0.01 | 0.02 ± 0.009 |
| S6 | 0.0096 ± 0.002 | 0.051 ± 0.02 | 1 ± 0.2 | 0.0037 ± 0.002 | 0.19 ± 0.03 | 0.039 ± 0.02 |
| S7 | 0.0024 ± 0.0004 | 0.048 ± 0.008 | 1 ± 0.08 | -0.0013 ± 0.0006 | 0.16 ± 0.01 | 0.047 ± 0.008 |

References

- Alfvin, R. L. and Fairchild, M. D. (1997). Observer variability in metameric color matches using color reproduction media. *Color Research & Application*, 22(3):530–539.
- Aronov, D., Nevers, R., and Tank, D. W. (2017). Mapping of a non-spatial dimension by the hippocampal–entorhinal circuit. *Nature*, 543(7647):719–722.
- Asano, Y., Fairchild, M. D., and Blondé, L. (2016a). Individual colorimetric observer model. *PLoS ONE*, 11(2):1–19.
- Asano, Y., Fairchild, M. D., Blondé, L., and Morvan, P. (2016b). Color matching experiment for highlighting interobserver variability. *Color Research and Application*, 41(15):530–539.
- Barlow, H. (2001). Redundancy reduction revisited. *Network: Computation in Neural Systems*, 12(3):241–253.
- Bellmund, J. L. S., Deuker, L., Schröder, T. N., and Doeller, C. F. (2016). Grid-cell representations in mental simulation. *Elife*, 5:e17089.
- Bellmund, J. L. S., Gärdenfors, P., Moser, E. I., and Doeller, C. F. (2018). Navigating cognition: Spatial codes for human thinking. *Science*, 362(6415):eaat6766.
- Chichilnisky, E. J. and Wandell, B. A. (1996). Seeing gray through the ON and OFF pathways. *Visual Neuroscience*, 13(3):591–596.
- Commission Internationale de l’Eclairage (1932). *Proceedings 1931*. Cambridge University Press, Cambridge.
- Constantinescu, A. O., O’Reilly, J. X., and Behrens, T. E. J. (2016). Organizing conceptual knowledge in humans with a gridlike code. *Science*, 352(6292):1464–1468.

- da Fonseca, M. and Samengo, I. (2016). Derivation of human chromatic discrimination ability from an information-theoretical notion of distance in color space. *Neural Computation*, 28(12):2628–2655.
- da Fonseca, M. and Samengo, I. (2018). Novel perceptually uniform chromatic space. *Neural Computation*, 30(6):1612–1623. PMID: 29566354.
- da Fonseca, M., Vattuone, N., Clavero, F., Echeveste, R., and Samengo, I. (2019). The subjective metric of remembered colors: A Fisher-information analysis of the geometry of human chromatic memory. *PLOS ONE*, 14:1–30.
- Derrington, A. M., Krauskopf, J., and Lennie, P. (1984). Chromatic mechanisms in lateral geniculate nucleus of macaque. *Journal of Physiology*, 357(1):241–265.
- Eichengreen, J. M. (1976). Unique hue loci: Induced shifts with complementary surrounds. *Vision Research*, 16(2):199–203.
- Ekroll, V., Faul, F., and Niederée, R. (2004). The peculiar nature of simultaneous colour contrast in uniform surrounds. *Vision Research*, 44(15):1765–1786.
- Fairchild, M. D. and Heckaman, R. L. (2013). Metameric observers: A Monte Carlo approach. *Color and Imaging Conference*, 2013(1):185–190.
- Fairchild, M. D. and Heckaman, R. L. (2016). Measuring observer metamerism: The Nimeroff approach. *Color Research & Application*, 41(2):115–124.
- Granata, D. and Carnevale, V. (2016). Accurate estimation of the intrinsic dimension using graph distances: Unraveling the geometric complexity of datasets. *Scientific Reports*, 6(1).
- Guild, J. (1932). The colorimetric properties of the spectrum. *Philosophical Transactions of the Royal Society of London A*, 230(681–693):6149–187.
- Hansen, T., Walter, S., and Gegenfurtner, K. R. (2007). Effects of spatial and temporal context on color categories and color constancy. *Journal of vision*, 7(4:2):1–15.
- Horner, A. H., Bisby, J. A., Zotow, E., Bush, D., and Burgess, N. (2018). Grid-like processing of imagined navigation. *Current Biology*, 26(6):842–847.
- Jameson, D. and Hurvich, L. M. (1964). Theory of brightness and color contrast in human vision. *Vision Research*, 4(1-2):135–154.
- Kaplan, R., Schuck, N. W., and Doeller, C. F. (2017). The role of mental maps in decision-making. *Trends in Neurosciences*, 40(5):256–259.

- Kellner, C. J. and Wachtler, T. (2016). Stimulus size dependence of hue changes induced by chromatic surrounds. *Journal of the Optical Society of America*, 33(3):A267–A272.
- Klauke, S. and Wachtler, T. (2015). “Tilt” in color space: Hue changes induced by chromatic surrounds. *Journal of Vision*, 15(13):1–11.
- Krauskopf, J. and Gegenfurtner, K. (1992). Color discrimination and adaptation. *Vision Research*, 32(11):2165–2175.
- Kumaran, D., Banino, A., Blundell, C., Hassabis, D., and Dayan, P. (2016). Computations underlying social hierarchy learning: Distinct neural mechanisms for updating and representing self-relevant information. *Neuron*, 92(5):1135–1147.
- MacAdam, D. L. (1942). Visual sensitivities to color differences in daylight. *Journal of the Optical Society of America*, 32(5):247–274.
- MacAdam, D. L. (1944). On the geometry of color space. *Journal of the Franklin Institute*, 238(5):195–201.
- Mayer, A., Mora, T., Rivoire, O., and Walczak, A. M. (2016). Diversity of immune strategies explained by adaptation to pathogen statistics. *PNAS*, 113(31):8630–8635.
- Provenzi, E. (2020). Geometry of color perception. part 1: structures and metrics of a homogeneous color space. *Journal of Mathematical Neuroscience*, 10(7).
- Radvanski, B. A. and Dombeck, D. A. (2018). An olfactory virtual reality system for mice. *Nature Communications*, 9(1):839.
- Resnikoff, H. L. (1974). Differential geometry and color perception. *Journal of Mathematical Biology*, 1:97–131.
- Schein, S. and Desimone, R. (1990). Spectral properties of v4 neurons in the macaque. *The Journal of Neuroscience*, 10(10):3369–3389.
- Schrödinger, E. (1920). Grundlinien einer Theorie der Farbenmetrik im Tagessehen. *Annalen der Physik*, 368(21):427–456.
- Silberstein, L. (1943). Investigations on the intrinsic properties of the color domain. *Journal of the Optical Society of America*, 33(1):1–10.
- Smith, V. C. and Pokorny (1996). Color contrast under controlled chromatic adaptation reveals opponent rectification. *Vision Research*, 36(19):3087–3105.

- Spall, J. C. (1998). Implementation of the simultaneous perturbation algorithm for stochastic optimization. *Aerospace and Electronic Systems, IEEE Transactions on, IEEE*, 34:817–823.
- Stiles, W. S. (1946). A modified Helmholtz line element in brightness-colour space. *Proceedings of the Physical Society*, 58(1):41–65.
- Stiles, W. S. and Burch, J. M. (1959). NPL colour-matching investigation: final report. *Journal of Modern Optics*, 6(1):1–26.
- Stockman, A. and Sharpe, L. T. (2000). Spectral sensitivities of the middle- and long-wavelength sensitive cones derived from measurements in observers of known genotype. *Vision Research*, 40(13):1711–1737.
- von Helmholtz, H. (1892). Kürzeste Linien im Farbensystem: Auszug aus einer Abhandlung gleichen Titels in Sitzgsber. der Akademie zu Berlin. 17. Dezember 1891. *Zeitschrift für Psychologie und Physiologie der Sinnesorgane*, 3:108–122.
- von Helmholtz, H. (1896). Physiological optics der Akademie zu Berlin. 17. Dezember 1891. *Vision Research*, 29:11:163–1647.
- Wachtler, T., Albright, T. D., and Sejnowski, T. J. (2001). Nonlocal interactions in color perception: nonlinear processing of chromatic signals from remote inducers. *Vision Research*, 12:1535–1546.
- Wachtler, T., Sejnowski, T. J., and Albright, T. D. (2003). Representation of color stimuli in awake macaque primary visual cortex. *Neuron*, 37(4):681–691.
- Ware, C. and Cowan, W. B. (1982). Changes in perceived color due to chromatic interactions. *Vision Research*, 22(11):1353–1362.
- Witzel, C. and Gegenfurtner, K. R. (2013). Categorical sensitivity to color differences. *Journal of Vision*, 13(7(1)):1–33.
- Wyszecki, G. and Fielder, G. H. (1971). New color-matching ellipses. *Journal of the Optical Society of America*, 61(9):1135–1152.
- Wyszecki, G. and Stiles, W. S. (1982). *Color Science: Concepts and Methods, Quantitative Data and Formulae*. Wiley, New York, 2 edition.
- Zeki, S. (1983). Colour coding in the cerebral cortex: The responses of wavelength-selective and colour-coded cells in monkey visual cortex to changes in wavelength composition. *Neuroscience*, 9(4):767–781.